AD-A076 115 NAVAL POSTGRADUATE SCHOOL MONTEREY CA F/G 10/2
PERFORMANCE ANALYSIS OF A TYPE OF ELECTROHYDRODYNAMIC POWER GEN--ETC(U
APR 79 T H GAWAIN , O BIBLARZ AFOSR-MIPR-78-0002
UNCLASSIFIED NPS67-79-006 NL

1 OF 1
AD A076115

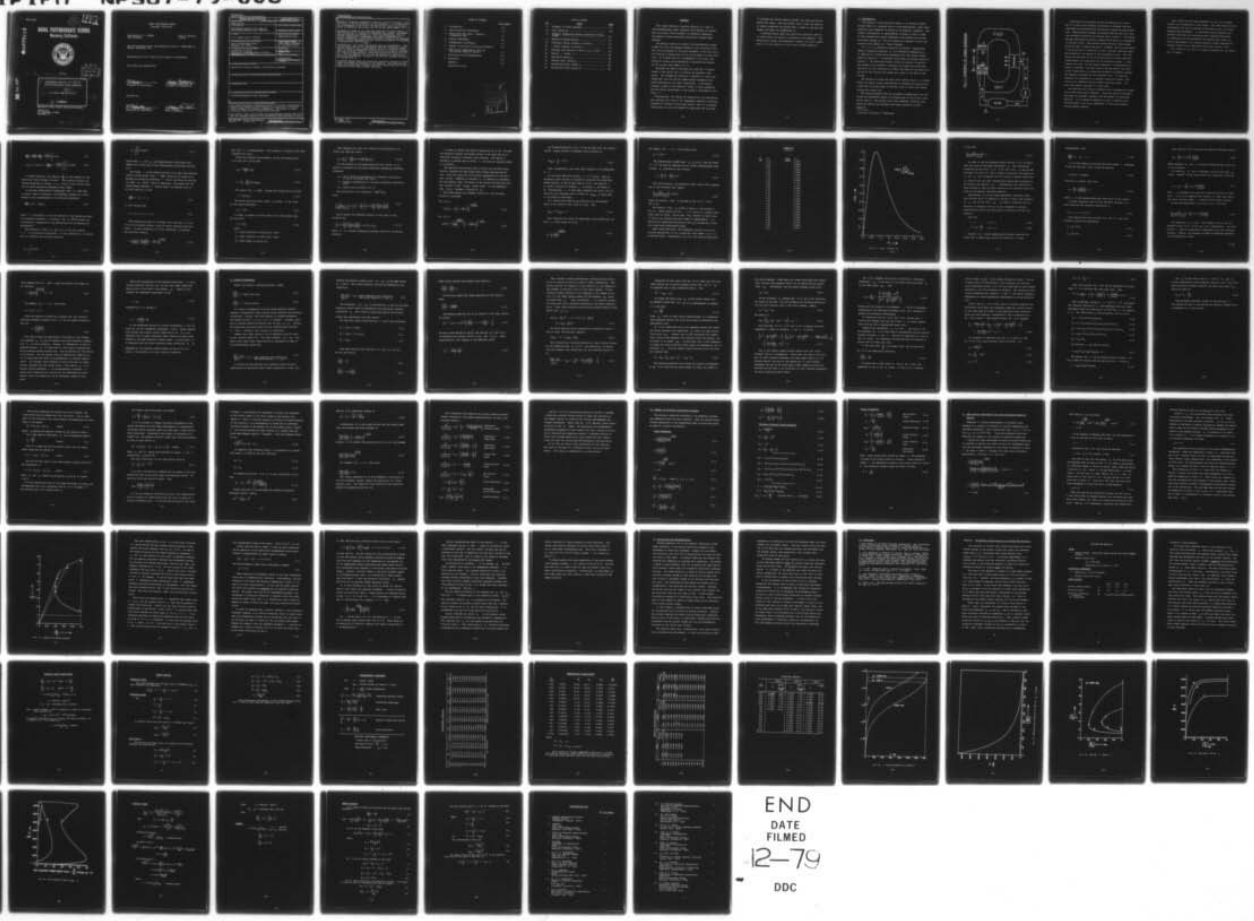

END
DATE FILMED
12-79
DDC

(14) NPS67-79-006

(2) Sc LEVEL II

AD A076115

NAVAL POSTGRADUATE SCHOOL

Monterey, California

(15) AFOSR-MIPR-78-0002,
ER-78-A-03-2122

(6) PERFORMANCE ANALYSIS OF A TYPE OF ELECTROHYDRODYNAMIC POWER GENERATOR,

(10) T.H. Gawain and O. Biblarz

(11) April 1979

(12) 91 p.

Approved for public release; distribution unlimited

Prepared for:
U.S. Department of Energy
Washington, DC

NAVAL POSTGRADUATE SCHOOL

Monterey, California

Rear Admiral T. F. Dedman
Superintendent

Jack R. Borsting
Provost

The work reported herein was supported by the U.S. Department of Energy, Washington, DC.

This report was prepared by:

T. H. Gawain

T. H. GAWAIN
Professor of Aeronautics

Oscar Biblarz

O. BIBLARZ, Associate
Professor of Aeronautics

Reviewed by:

M. F. Platzer per WG

M. F. PLATZER, Chairman
Department of Aeronautics

William M. Tolles

W. M. TOLLES
Dean of Research

UNCLASSIFIED

SECURITY CLASSIFICATION OF THIS PAGE (When Data Entered)

REPORT DOCUMENTATION PAGE		READ INSTRUCTIONS BEFORE COMPLETING FORM
1. REPORT NUMBER NPS67-79-006	2. GOVT ACCESSION NO.	3. RECIPIENT'S CATALOG NUMBER
4. TITLE (and Subtitle) Performance Analysis of a Type of Electrohydrodynamic Power Generator		5. TYPE OF REPORT & PERIOD COVERED 6. PERFORMING ORG. REPORT NUMBER
7. AUTHOR(s) T. H. Gawain and O. Biblarz		8. CONTRACT OR GRANT NUMBER(s) AFOSR-MIPR-78-0002
9. PERFORMING ORGANIZATION NAME AND ADDRESS Naval Postgraduate School Monterey, CA 93940		10. PROGRAM ELEMENT, PROJECT, TASK AREA & WORK UNIT NUMBERS Inter Agency Agreement No. ER-78-A-03-2122
11. CONTROLLING OFFICE NAME AND ADDRESS Department of Energy Division of Advanced Energy Projects Washington, DC 20545		12. REPORT DATE April 1979 13. NUMBER OF PAGES 83
14. MONITORING AGENCY NAME & ADDRESS(if different from Controlling Office)		15. SECURITY CLASS. (of this report) Unclassified 15a. DECLASSIFICATION/DOWNGRADING SCHEDULE

16. DISTRIBUTION STATEMENT (of this Report)

Approved for public release; distribution unlimited

17. DISTRIBUTION STATEMENT (of the abstract entered in Block 20, if different from Report)

18. SUPPLEMENTARY NOTES

19. KEY WORDS (Continue on reverse side if necessary and identify by block number)

Electrohydrodynamic Power Generator

20. ABSTRACT (Continue on reverse side if necessary and identify by block number)

This report develops a detailed analysis of a type of electrohydrodynamic power generator which employs an ejector and a so-called "fluid flywheel" as essential components. The medium is steam containing electrically charged water droplets.

The analysis takes into account the experimentally established facts that the maximum strength of the electrical field that can be sus-

DD FORM 1 JAN 73 1473 EDITION OF 1 NOV 65 IS OBSOLETE
S/N 0102-014-6601 |

UNCLASSIFIED
SECURITY CLASSIFICATION OF THIS PAGE (When Data Entered)

tained at incipient breakdown at the most critical location is proportional to the fluid density at that location. It is shown that as a consequence of this fact, the electrical output can be maximized by designing the primary jet for an exit Mach number of 0.71.

Estimates are made of the pump work required, of mixing losses in the ejector and of friction and secondary flow losses. The mathematical analysis is reduced to a fully non-dimensional form and the key dimensionless parameters that govern performance are clearly identified. A preliminary estimate is made of the numerical values of these parameters and the overall performance of the system is estimated on this basis.

Unfortunately, the results so obtained are very pessimistic. They indicate that even at 100 atmospheres pressure, electrical breakdown so severely limits power output, that it is probably insufficient to cover the demand for pump power and for power to overcome the various losses involved, let alone provide any useful net output. The only hopeful note is that the analysis so clearly pinpoints the problem that it might in the end also suggest the means for surmounting it.

A modified design where the electrical conversion section is placed after the ejector is analyzed in the Appendix. This modification yields less pessimistic results, but still leaves doubt as to the viability of this type of power generator.

TABLE OF CONTENTS

LIST OF FIGURES

ABSTRACT

This report develops a detailed analysis of a type of electrohydrodynamic power generator which employs an ejector and a so-called "fluid flywheel" as essential components. The medium is steam containing electrically charged water droplets.

The analysis takes into account the experimentally established fact that the maximum strength of the electrical field that can be sustained at incipient breakdown at the most critical location is proportional to the fluid density at that location. It is shown that as a consequence of this fact, the electrical output can be maximized by designing the primary jet for an exit Mach number of 0.71.

Estimates are made of the pump work required, of mixing losses in the ejector and of friction and secondary flow losses. The mathematical analysis is reduced to a fully non-dimensional form and the key dimensionless parameters that govern performance are clearly identified. A preliminary estimate is made of the numerical values of these parameters and the overall performance of the system is estimated on this basis.

Unfortunately, the results so obtained are very pessimistic. They indicate that even at 100 atmospheres pressure, electrical breakdown so severely limits power output, that it is probably insufficient to cover the demand for pump power and for power

to overcome the various losses involved, let alone provide any useful net output. The only hopeful note is that the analysis so clearly pinpoints the problem that it might in the end also suggest the means for surmounting it.

A modified design where the electrical conversion section is placed after the ejector is analysed in the Appendix. This modification yields less pessimistic results, but still leaves doubt as to the viability of this type of power generator.

1. Introduction

The purpose of this analytical report is to develop a mathematical model of a proposed type of electrohydrodynamic (EHD) power generator which embodies an ejector as an essential component. The overall configuration is approximately toroidal in form in order to help conserve the angular momentum of the working fluid which circulates through it. For this reason the inventor* of this configuration has dubbed it a "fluid flywheel".

Fig. 1.1 is a schematic diagram of the device. Superheated steam at stagnation pressure p_o and stagnation temperature T_o is supplied to a nozzle which discharges into the ejector mixing region at station 1. A secondary fluid enters the mixing region at station 2. The resulting mixture leaves the ejector at station 3. The ejector action creates a pressure rise across the mixing section which is just sufficient to offset the effect of the power output and of the various flow losses that occur in the rest of the circuit.

The mixture of liquid and vapor which leaves station 3 is cooled during its return circuit sufficiently to condense and separate out a mass flow of liquid equal to the mass flow of steam which passes through the primary jet.

The liquid withdrawn from the condenser is pumped back into the boiler and superheater where it is heated back to the initial stagnation state 0. The primary fluid thus undergoes a Rankine cycle where the turbine and condenser have been replaced by an EHD generator.

---

* See note in Section 9, References.

Fig. 1.1 SCHEMATIC OF POWER GENERATOR

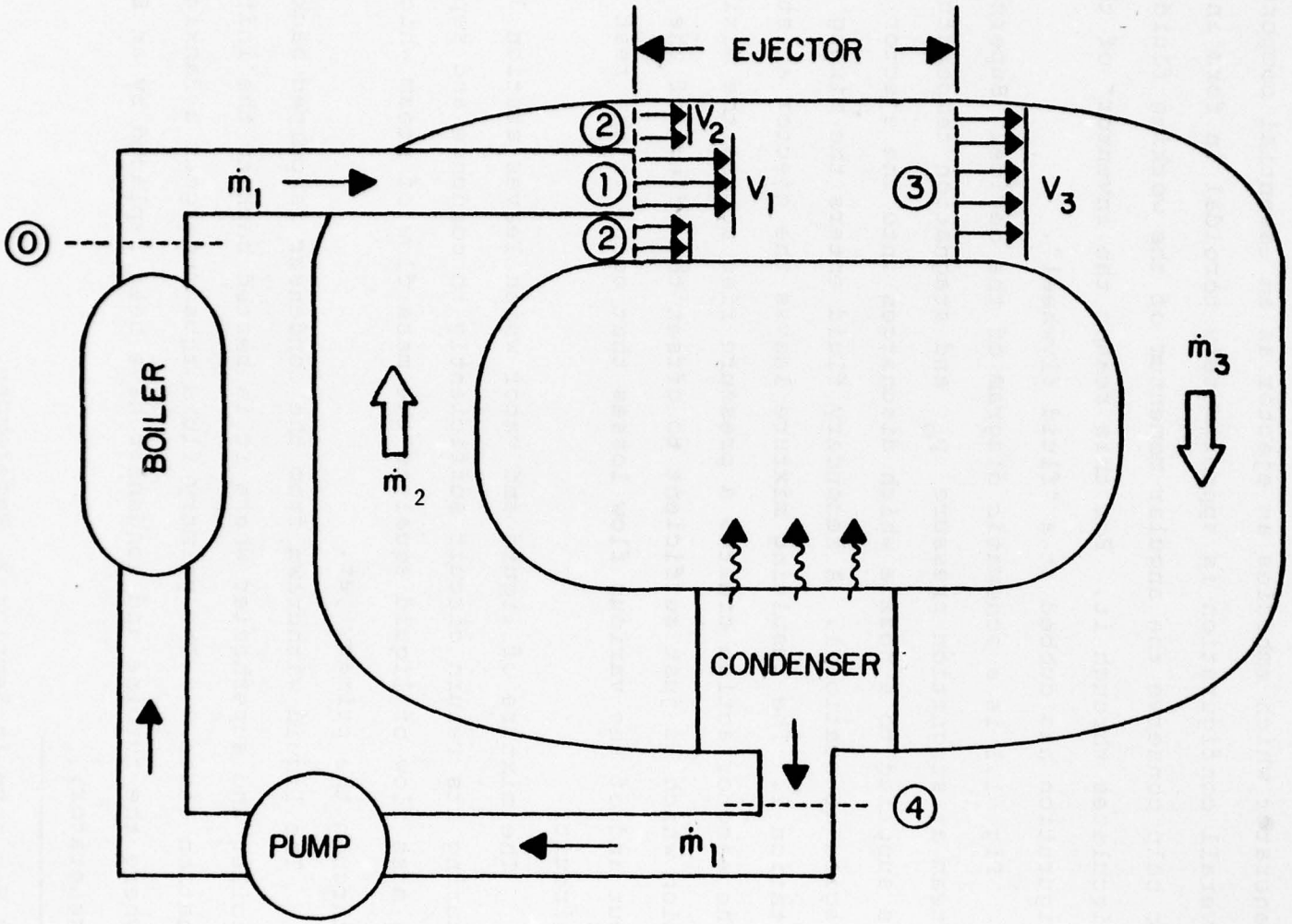

Conditions in the primary nozzle are controlled in such a way as to cause fine droplets of moisture to condense here and electrodes are provided which electrically charge the liquid droplets. These electric charges are removed from the flow by a grid type collector located at the ejector exit, station 3. The moving charges constitute an electric current which sets up a corresponding electric field. The electric forces acting on the charged particles tend to oppose the motion. However, the size and charge of the particles is controlled in such a way that they have negligible mobility with respect to the surrounding fluid. Thus the moving gas does work on the fluid particles in moving them downstream against the resistance of the electrical forces. In performing this work, the gas stream undergoes a corresponding decrease in enthalpy. The work done by the gas against the electrical forces sets up an electrical potential difference between the charging electrode and the collector grid. If these two terminals be connected by an external electrical circuit, that circuit will therefore deliver useful electrical power. The only turbo device required is a small pump.

The question that arises is whether such a hypothetical scheme can be made practically effective. There are various formidable obstacles to overcome, including the achievement of negligible mobility. It is therefore important to have a complete quantitative model of all cycle components to help guide research and development efforts.

Such a model has now been developed for the fluid flywheel concept and is presented in this report. The model shows that the performance that can be attained is governed by just a few basic dimensionless parameters. It identifies these parameters and provides some basis for estimating their probable magnitudes. By identifying the key parameters and showing their effect on overall performance, this analysis permits current experimental research efforts to be redirected along more fruitful lines.

This report is the result of research sponsored by the Department of Energy.

2. Basic Electrical Performance

It is convenient in the present analysis to introduce a parameter σ which is used to distinguish between the two distinct cases of positively and negatively charged particles. Specifically, we set $\sigma = +1$ for the case of positively charged particles, and we set $\sigma = -1$ for the case of negatively charged particles. It is then appropriate to denote the electrical charge per unit mass by the product σq where q has the units of coulombs/kg and is always positive by definition.

The electrical working section of the generator coincides with the mixing region of the ejector and, assuming polar symmetry, the distribution of q is essentially two dimensional over this region. However, our purpose in the present section is to develop certain key dimensionless parameters which depend primarily on how q varies with respect to the axial coordinate z. These parameters are not sensitive to variation with respect to the radial coordinate r. Under these circumstances it is permissible to simplify the analysis in the following way: At each axial station z that lies within the mixing region, we subdivide the total cross-sectional area A into an inner circular region of area A' and an outer concentric annulus of area A'' such that

$$A' + A'' = A = A_3 = \text{constant along channel} \qquad (2.1)$$

While fluid density ρ (kg/m) is treated as essentially uniform over the entire mixing region, the axial velocity (m/sec) is

assumed to have the value V' over the inner area A' and the value $V'' = V_2$ over the outer annular area A''. Similarly, charge density (coulomb/kg) is assumed to have the value q' over the inner area A' and the value $q'' = 0$ over the outer annular area A''. Moreover, the quantities A', V' and q' are regarded as functions of coordinate z which vary monotonically from their initial values A_1, V_1, q_1 at $z = 0$ to their final values A_3, V_3, q_3 at $z = 1$. The exact form of these functions is not of immediate importance in the present development.

It is useful to introduce the following auxiliary definitions at this point on

ℓ = length of working section, m

V = magnitude of voltage change across working section, positive by definition, volts

$\varepsilon = \varepsilon_o$ = permittivity of free space
$= 8.854 \times 10^{-12}$ farad/m

ϕ = electric potential, volts

$f = \frac{\phi}{V}$ = dimensionless electric potential

$\zeta = \frac{z}{\ell}$ = dimensionless axial coordinate

$g = \frac{q'}{q_1}$ = dimensionless charge/mass ratio

Poisson's equation and its first two integrals can now be represented in the following one dimensional version:

$$\left(\frac{d^2\phi}{dz^2}\right) = \frac{V}{\ell^2}\left(\frac{d^2 f}{d\zeta^2}\right) = -\frac{\sigma\rho_1 q_1}{\varepsilon} g(\zeta) \qquad (2.2)$$

$$\left(\frac{d\phi}{dz}\right) = \frac{V}{\ell}\left(\frac{df}{d\zeta}\right) = \left(\frac{d\phi}{dz}\right)_o - \frac{\sigma\rho_1 q_1 \ell}{\varepsilon}\int_0^\zeta g(\zeta)\,d\zeta \tag{2.3}$$

$$(\phi-\phi_o) = V(f-f_o) = \left(\frac{d\phi}{dz}\right)_o \ell\zeta - \frac{\sigma\rho_1 q_1 \ell^2}{\varepsilon}\int_0^\zeta\int_0^\zeta g(\zeta)\,d\zeta d\zeta \tag{2.4}$$

In these equations, the quantity $\frac{d\phi}{dz}$ is the negative of the electrical field strength (volts/m). This quantity attains its maximum magnitude at station $z = 0$, which is the critical location at which electrical breakdown first occurs.

It has been established by experiment, Ref. (1), that over a certain range of pressures, the breakdown strength of a given medium is well approximated by the following expression

$$\left(\frac{d\phi}{dz}\right)_o = \sigma\left[C_o + C_B R\rho_1\right] \tag{2.5}$$

where R (joules/kg^oK) is the gas constant of the medium and where the breakdown constants C_o (volts/m) and C_B ($m^2{}^oK$/coulomb) are characteristic properties of the medium which can be measured experimentally.

The evaluation of Eqs (2.3) and (2.4) at the exit station $\zeta = 1$ is of particular importance. In this connection it is convenient to introduce the following notation:

$$\psi_1 = \int_0^1 g(\zeta)\,d\zeta \tag{2.6}$$

$$\psi_2 = \int_0^1 \int_0^\zeta g(\zeta)\, d\zeta d\zeta \tag{2.7}$$

Notice that ψ_1 and ψ_2 are dimensionless coefficients that depend only on the form of the dimensionless charge/mass function $g(\zeta)$.

The length ℓ of the working section of an ideal EHD generator having a given current flow i (amps) should be so chosen as to maximum the potential difference V (volts) and hence the electrical power P_e (watts) which is generated. This means that the dimensionless potential f should attain its maximum value at the exit station, or that

$$\left(\frac{df}{d\zeta}\right) = 0 \quad \text{at} \quad \zeta = 1 \tag{2.8}$$

It also follows that

$$(f - f_o) = \sigma \quad \text{at} \quad \zeta = 1 \tag{2.9}$$

Upon substituting Eqs (2.5) through (2.9) into Eqs (2.3) and (2.4) we can readily extract a pair of useful relations from the result. In this connection it is also convenient to introduce the auxiliary notation

$$\alpha = \left(\frac{C_o}{C_B R \rho_1}\right) = \frac{C_o}{C_B}\left(\frac{T_o}{p_o}\right)\left[1 + \frac{\gamma-1}{2} M_1^2\right]^{\frac{1}{(\gamma-1)}} \tag{2.10}$$

Note that α is dimensionless. This quantity is normally very small compared with unity.

Using this notation and procedure, we may now summarize Eqs (2.3) and (2.4) in the form

$$q_1 \ell = \frac{(1+\alpha)}{\psi_1} \varepsilon C_B R \tag{2.11}$$

$$V = \left(1 - \frac{\psi_2}{\psi_1}\right)(1+\alpha) C_B R \rho_1 \ell \tag{2.12}$$

The current flow i (amps) through the channel may be written

$$i = \sigma q_1 \rho_1 V_1 A_1 \tag{2.13}$$

The gross electrical power output P_e (watts) is now given by the simple expression

$$P_e = [\sigma V] i \tag{2.14}$$

In order to reduce our final result into a more useful form we also write

$$V_1 = a_1 M_1 \tag{2.15}$$

where

V_1 = axial velocity to nozzle exit, m/sec

a_1 = sonic velocity at nozzle exit, m/sec

M_1 = Mach number at nozzle exit

Upon combining the last five relations and rearranging, we obtain the important result

$$P_e = \frac{1}{\psi_1}\left(1 - \frac{\psi_2}{\psi_1}\right)(1+\alpha)^2 \varepsilon C_B^2 R^2 \rho_1^2 a_1 M_1 A_1 \tag{2.16}$$

For the purpose of non-dimensionalizing this result, it is useful to introduce the following additional dimensional reference parameters

a_o = sonic velocity corresponding to stagnation conditions at inlet to primary jet, m/sec

ρ_o = density corresponding to the above stagnation conditions, kg/m^3

A_t = throat area of primary jet, m^2

Now dividing Eq (2.16) through by $\varepsilon C_B^2 R^2 \rho_o^2 a_o A_t$ gives

$$\left(\frac{P_e}{\varepsilon C_B^2 R^2 \rho_o^2 a_o A_t}\right) = \frac{1}{\psi_1}\left(1 - \frac{\psi_2}{\psi_1}\right)\left\{(1+\alpha)^2\left(\frac{\rho_1}{\rho_o}\right)^2\left(\frac{a_1}{a_o}\right)M_1\left(\frac{A_1}{A_t}\right)\right\} \tag{2.17}$$

Let us denote the bracketed quantity on the right in the following way

$$\left\{(1+\alpha)^2\left(\frac{\rho_1}{\rho_o}\right)^2\left(\frac{a_1}{a_o}\right)M_1\left(\frac{A_1}{A_t}\right)\right\} = (1+\alpha)^2 \psi_3 F(M_1) \tag{2.18}$$

where ψ_3 is a certain normalizing constant which will be defined presently.

In order to analyze the function defined by Eq (2.18), we treat the expansion through the primary nozzle in the usual way as an isentropic process of constant total enthalpy. The medium is treated as a perfect gas for which γ, the ratio of specific heats, is a constant.

The relations which govern such a nozzle flow are well known and will therefore be used freely here without detailed derivation. Note that there are two distinct expressions for the function $\psi_3 F(M_1)$ depending on whether M_1 is subsonic or supersonic. For the subsonic case, the throat of the nozzle coincides with the exit station so that (A_1/A_t) equals unity. In the supersonic case (A_1/A_t) becomes a function of M_1.

When these details are properly worked out, the following solution is obtained.

For $M_1 \leq 1$

$$\psi_3 F(M_1) = M_1 \left[1 + \frac{\gamma-1}{2} M_1^2\right]^{-\frac{(\gamma+3)}{2(\gamma-1)}} \tag{2.19}$$

For $M_1 \geq 1$

$$\psi_3 F(M_1) = \left[\frac{2}{\gamma+1}\right]^{\frac{(\gamma+1)}{2(\gamma-1)}} \left[1 + \left(\frac{\gamma-1}{2}\right) M_1^2\right]^{-\frac{1}{(\gamma-1)}} \tag{2.20}$$

By differentiating Eq (2.19), it can be shown that the function $\psi_3 F(M_1)$ passes through its maximum value precisely at

$$M_{1opt} = \frac{1}{\sqrt{2}} \doteq 0.71 \tag{2.21}$$

Note, incidentally, that this result happens to be independent of γ!

On the other hand the function $(1 + \alpha)^2 \psi_3 F(M_1)$ does not necessarily pass through its maximum at precisely this same Mach number because, as may be seen from Eq (2.10), the quantity α is itself a function of density ρ at station 1, and hence of M_1. Nevertheless, α is very small compared with unity, and its variation will therefore have an effect on M_{1opt} so small that it can safely be neglected.

As a normalizing condition we stipulate that the maximum value of the function $F(M_1)$ shall be unity. Thus

$$F_{max} = F(M_{1opt}) = 1 \tag{2.22}$$

This constraint now fixes the magnitude of the normalizing constant ψ_3 which works out to be

$$\psi_3 = \frac{1}{\sqrt{2}} \left[\frac{4}{\gamma+3}\right]^{\frac{(\gamma+3)}{2(\gamma-1)}} \tag{2.23}$$

For example, for $\gamma = 1.3$ this formula gives

$$\psi_3 = 0.4211 \tag{2.24}$$

The dimensionless coefficients ψ_1, ψ_2 and ψ_3 and the factor $(1 + \alpha)^2$ can next be combined into an overall dimensionless coefficient ψ_4 according to the relation

$$\psi_4 = \frac{\psi_3}{\psi_1}\left(1 - \frac{\psi_2}{\psi_1}\right)(1+\alpha)^2 \tag{2.25}$$

With this notation, the electrical power output can be expressed in the following form, namely,

$$\left(\frac{P_e}{\varepsilon C_B{}^2 R^2 \rho_o{}^2 a_o A_t}\right) = \psi_4 F(M_1) \tag{2.26}$$

where the function $F(M_1)$ is defined by Eqs (2.19), (2.20) and (2.23).

The function $F(M_1)$ is listed in Table 2.1 and plotted in Fig 2.1. These results are for $\gamma = 1.3$ which is a typical value often used for steam. Notice that $F(M_1)$ reaches its peak value of unity at an optimum exit Mach number of approximately 0.71. Observe that appreciable deviations from this optimum exit condition cause heavy performance losses.

Under these conditions, the subsequent analysis will be restricted specifically to the optimum exit Mach number $M_1 = 0.71$ as derived above. Consequently, Eq (2.25) can then be simplified

TABLE 2.1

$\gamma = 1.3$

M_1	$F(M_1)$
0.0	0.0
0.20	0.4550
0.40	0.8014
0.60	0.9774
0.71	1.0000
0.80	0.9849
1.00	0.8722
1.20	0.7241
1.40	0.5886
1.60	0.4704
1.80	0.3711
2.00	0.2901
2.20	0.2253
2.40	0.1744
2.60	0.1347
2.80	0.1041
3.00	0.0805
3.20	0.0625
3.40	0.0486
3.60	0.0380
3.80	0.0298
4.00	0.0235
4.20	0.0186
4.40	0.0148
4.60	0.0119
4.80	0.0095
5.00	0.0077

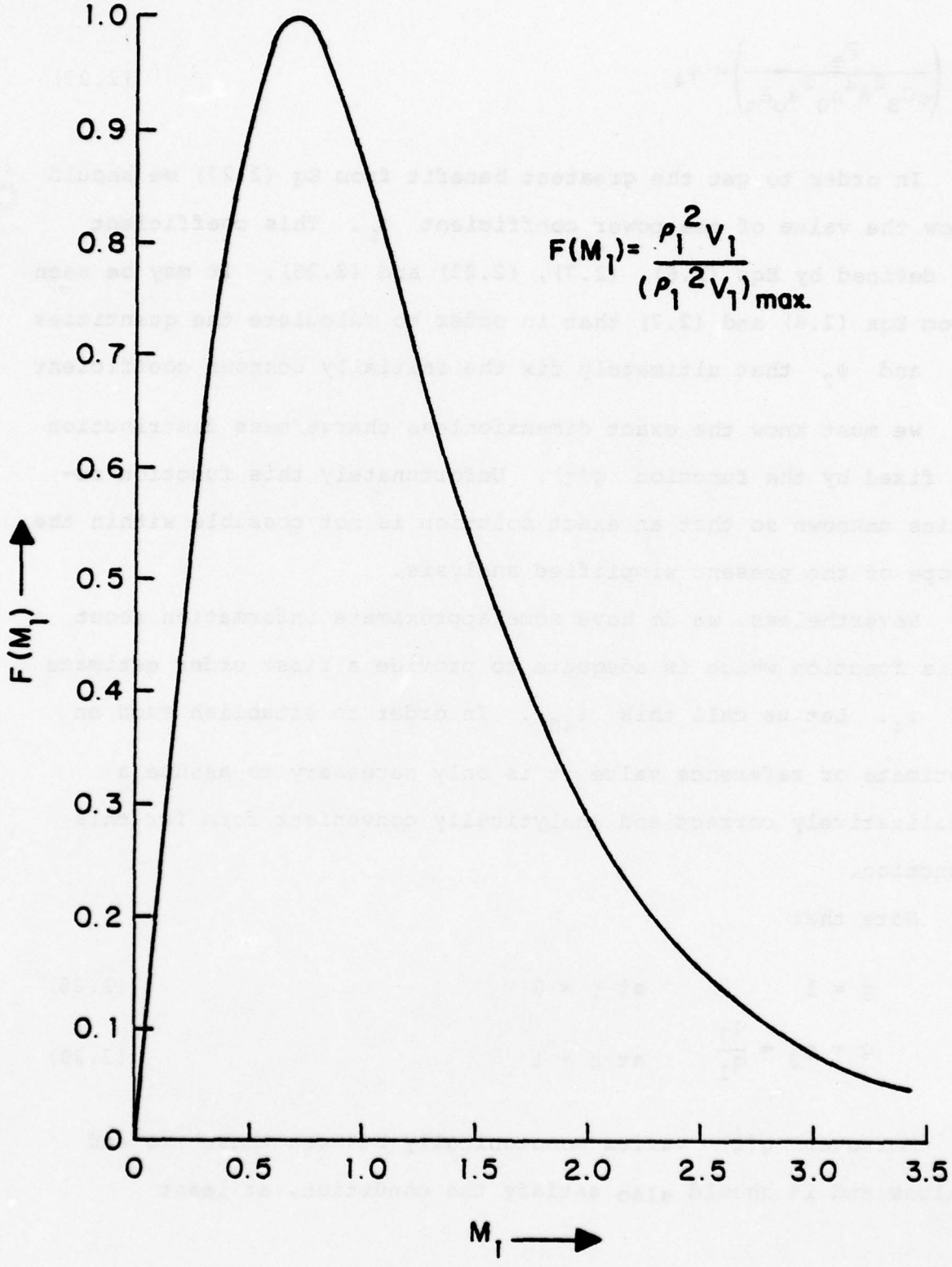

Fig. 2.1 $F(M_1)$ versus M_1

to the form

$$\left(\frac{P_e}{\varepsilon C_B{}^2 R^2 \rho_0{}^2 a_o A_t}\right) = \psi_4 \qquad (2.27)$$

In order to get the greatest benefit from Eq (2.27) we should know the value of the power coefficient ψ_4. This coefficient is defined by Eqs (2.6), (2.7), (2.23) and (2.25). It may be seen from Eqs (2.6) and (2.7) that in order to calculate the quantities ψ_1 and ψ_2 that ultimately fix the initially unknown coefficient ψ_4, we must know the exact dimensionless charge/mass distribution as fixed by the function $g(\zeta)$. Unfortunately this function remains unknown so that an exact solution is not possible within the scope of the present simplified analysis.

Nevertheless, we do have some approximate information about this function which is adequate to provide a first order estimate of ψ_4. Let us call this ψ_{40}. In order to establish such an estimate or reference value it is only necessary to assume a qualitatively correct and analytically convenient form for this function.

Note that

$$g = 1 \qquad \text{at } \zeta = 0 \qquad (2.28)$$

$$g = g_3 = \frac{q_3}{q_1} \qquad \text{at } \zeta = 1 \qquad (2.29)$$

Moreover $g(\zeta)$ varies monotonically between these two end values and it should also satisfy the condition, at least

approximately, that

$$\left(\frac{dg}{d\zeta}\right) = 0 \quad \text{at} \quad \zeta = 1 \tag{2.30}$$

It is also timely to note here that the current i evaluated at the two stations 1 and 3 gives the relation

$$q_1\rho_1 A_1 V_1 = q_3\rho_3 A_3 V_3 \tag{2.31}$$

From this we readily infer that

$$g_3 = \frac{q_3}{q_1} = \left(\frac{\rho_1 A_1 V_1}{\rho_3 A_3 V_3}\right) = x \tag{2.32}$$

where x is the dimensionless mass flow ratio of the ejector.

A simple analytical form for the reference function $g(\zeta)$ that satisfies the foregoing constraints is

$$g(\zeta) = x + (1-x)(1-\zeta)^2 \tag{2.33}$$

Upon substituting this into Eqs (2.6) and (2.7) and integrating we obtain the expressions

$$\psi_1 = \frac{1}{3}(1+2x) \tag{2.34}$$

$$\psi_2 = \frac{1}{4}(1+x) \tag{2.35}$$

Then using Eq (2.25) we obtain the desired reference value as

$$\psi_{40} = \left[\frac{3}{4}\,\psi_3(1+\alpha)^2\right]\,\frac{(1+5x)}{(1+2x)^2} \tag{2.36}$$

where constants ψ_3 and α are still defined by Eqs (2.23) and (2.10) as before.

Of course ψ_{40} is only a reference, not the true value ψ_4 itself. However, we may relate these two quantities as follows.

$$\psi_4 = \mu\psi_{40} = \mu\left[\frac{3}{4}\,\psi_3(1+\alpha)^2\right]\frac{(1+5x)}{(1+2x)^2} \tag{2.37}$$

Here μ is regarded as an empirical correction factor of order unity. It is to be expected that whereas ψ_4 itself may tend to vary over a certain range, μ should be more nearly constant.

We may now combine Eqs (2.27) and (2.37) in the form

$$\left(\frac{P_e}{\varepsilon C_B^{\,2} R^2 \rho_o^{\,2} a_o A_t}\right) = \mu\left[\frac{3}{4}\,\psi_3(1+\alpha)^2\right]\frac{(1+5x)}{(1+2x)^2} \tag{2.38}$$

The quantities ψ_3, α and x which appear in Eq (2.38) are defined by Eqs (2.23), (2.10) and (2.32), respectively. The coefficient μ must be determined by experiment or by more advanced analysis. However, for purposes of order of magnitude estimates it is permissible to take

$$\mu = 1 \tag{2.39}$$

3. Gross Electrical Power: Change of Dimensional Base

In analyzing the mixing and friction losses in the ejector and the friction and secondary losses in other parts of the system, it will prove useful to employ as dimensional reference quantities the fluid density $\rho = \rho_1 = \rho_2 = \rho_3$ in the ejector, the exit area A_3 from the ejector and the average axial velocity V_3 at this station. Thus the reference mass flow rate becomes $\rho_3 A_3 V_3$ (kg/sec), the reference kinetic energy per unit mass becomes $V_3^2/2$ (joule/kg) and the reference power becomes $(\rho_3 A_3 V_3)\ (V_3^2/2)$ (watts). In this connection it is appropriate to define a dimensionless gross electrical power coefficient c_e in the following way, namely,

$$c_e = \frac{P_e}{\left[\rho_3 A_3 V_3\right]\left[V_3^2/2\right]} \tag{3.1}$$

It is also necessary to establish suitable links between the above reference quantities and certain corresponding quantities at station 1, the exit from the primary jet. In this connection recall that

$$\left(\frac{\dot{m}_1}{\dot{m}_3}\right) = \left(\frac{\rho_1 A_1 V_1}{\rho_3 A_3 V_3}\right) = x = \text{dimensionless mass flow ratio} \tag{3.2}$$

We also elect to introduce the following definition

$$\left(\frac{V_1}{V_3}\right) = y = \text{dimensionless velocity ratio} \tag{3.3}$$

As before it will be convenient to write

$$V_1 = a_1 M_1 \tag{3.4}$$

Moreover we can substitute for P_e in Eq (3.1) its expression as previously developed in Eq (2.38).

When the foregoing relations are combined and rearranged, the following result is obtained

$$c_e = \mu \left\{ \frac{\frac{3}{4} \frac{\psi_3}{\gamma} (1+\alpha)^2}{\frac{1}{2}\left(\frac{\rho_1}{\rho_o}\right)\left(\frac{a_1}{a_o}\right)^3 M_1^3 \left(\frac{A_1}{A_t}\right)} \right\} \left\{ \frac{\gamma \varepsilon C_B^2 R^2 \rho_o}{a_o^2} \right\} \left\{ \frac{(1+5x)xy^2}{(1+2x)^2} \right\} \tag{3.5}$$

This suggest the utility of defining the following auxiliary quantities, namely,

$$\psi = \left\{ \frac{\frac{3}{4} \frac{\psi_3}{\gamma} (1+\alpha)^2}{\frac{1}{2}\left(\frac{\rho_1}{\rho_o}\right)\left(\frac{a_1}{a_o}\right)^3 M_1^3 \left(\frac{A_1}{A_t}\right)} \right\} \tag{3.6}$$

and

$$\beta = \left\{ \frac{\gamma \varepsilon C_B^2 R^2 \rho_o}{a_o^2} \right\} \tag{3.7}$$

Recall that the quantities involved in Eq (3.6) all correspond to the value $M_{1opt} = 1/\sqrt{2}$. Hence ψ turns out to be a constant

which depends only on γ and α. When the details are worked out we find that

$$\psi = \frac{3}{\gamma}\left[\frac{4}{\gamma + 3}\right]^{\left(\frac{\gamma + 1}{\gamma - 1}\right)} (1 + \alpha)^2 \tag{3.8}$$

For example, for $\gamma = 1.3$ this gives

$$\psi = 1.32(1 + \alpha)^2 \tag{3.9}$$

Since the medium is treated as a perfect gas, the crucially important parameter defined by Eq (3.7) can be further reduced to the form

$$\beta = \left(\frac{\varepsilon C_B^{\,2} p_o}{T_o^{\,2}}\right) \tag{3.10}$$

This result shows the importance of maintaining inlet stagnation pressure p_o as high as possible and inlet stagnation temperature T_o as low as possible. However, if condensation is used to produce droplets, T_o is restricted to that range of temperatures which produces optimum droplet size. One way around this restriction is as follows: Let the carrier fluid be changed from steam to air (or to some other gas which is noncondensible at ordinary temperatures). Let charged liquid droplets or solid particles of proper size be injected into the carrier fluid. This permits T_o to be sharply reduced whereupon β is correspondingly increased. Of course this alternative may involve its own characteristic drawbacks as well, but these will not be discussed further at this point.

While the introduction of the separate quantities μ, ψ and β follows naturally from Eq (3.5), we note that these quantities always occur in the form of the product $\mu\psi\beta$. Hence it will simplify the subsequent development to set

$$\upsilon = \mu\psi\beta \tag{3.11}$$

whereupon Eq (3.5) reduces to

$$c_e = \upsilon \frac{(1+5x)}{(1+2x)^2} xy^2 \tag{3.12}$$

In the subsequent analysis of ejector performance, it will be shown how the two fundamental parameters x and y govern pressure rise through the ejector, mixing losses and so on. Eq (3.12) therefore ties in gross electrical power output with these other effects on the same consistent overall basis. In particular, it is important that the gross electrical power coefficient c_e as expressed by this equation should exceed the sum of all the losses in the system by as wide a margin as possible.

4. Ejector Performance

Recall the notation introduced earlier, namely,

$$\left(\frac{\dot{m}_1}{\dot{m}_3}\right) = x = \text{mass flow ratio} \tag{4.1}$$

$$\left(\frac{V_1}{V_3}\right) = y = \text{velocity ratio} \tag{4.2}$$

As a basis of comparison with the actual physical ejector, consider a hypothetical ideal ejector which satisfies the following constraints. Firstly, the fluid density is uniform throughout the ejector so that $\rho_1 = \rho_2 = \rho_3 = \rho$ = constant. Secondly, pressure is uniform across the entire inlet so that $p_2 = p_1$. Thirdly, the velocities are purely axial and are uniform across sections 1, 2 and 3. Fourthly, wall friction is negligible.

Imagine this ideal ejector to be in operation with all electrical circuits turned off. The ideal pressure $(p_3^* - p_1)$ that would occur under these conditions may be expressed by means of the dimensionless coefficient

$$\frac{(p_3^* - p_1)}{\frac{1}{2}\rho V_3^2} = c_p^* = \text{ideal pressure rise coefficient (for given values of } x \text{ and } y) \tag{4.3}$$

Of course the real physical unit operating under realistic conditions with electrical power output connected to a load, will

produce some smaller pressure rise $(p_3 - p_1)$ at the same values of x and y. This actual pressure rise may be expressed by the coefficient

$$\frac{(p_3 - p_1)}{\frac{1}{2}\rho V_3^2} = c_p = \text{actual pressure rise coefficient (for given values of } x \text{ and } y) \tag{4.4}$$

The difference $(c_p^* - c_p)$ is accounted for in part by the gross electrical power output as expressed by the previously analyzed coefficient c_e and in part by additional mixing and friction losses that characterize the real system.

The mass flow rates across sections 1, 2 and 3 may be written

$$\dot{m}_1 = \rho A_1 V_1 = x\rho A_3 V_3 \tag{4.5}$$

$$\dot{m}_2 = \rho A_2 V_2 = (1-x)\, A_3 V_3 \tag{4.6}$$

$$\dot{m}_3 = \rho A_3 V_3 \tag{4.7}$$

From these relations and from Eqs (4.1) and (4.2) we find the two area ratios

$$\left(\frac{A_1}{A_3}\right) = \frac{x}{y} \tag{4.8}$$

$$\left(\frac{A_2}{A_3}\right) = (1-x)\left(\frac{V_3}{V_2}\right) \tag{4.9}$$

These ratios satisfy the constant area condition

$$\left(\frac{A_1}{A_3}\right) + \left(\frac{A_2}{A_3}\right) = 1 \tag{4.10}$$

We can solve these last three equations for the velocity ratio

$$\left(\frac{V_2}{V_3}\right) = \frac{(1-x)y}{(y-x)} \tag{4.11}$$

The momentum equation can now be applied to the ideal ejector as follows

$$(p_3^* - p_1)A_3 = \rho A_3 V_3^2 \left\{ x\left(\frac{V_1}{V_3}\right) + (1 - x)\left(\frac{V_2}{V_3}\right) - 1 \right\} \tag{4.12}$$

We next divide through by $\frac{1}{2}\rho A_3 V_3^2$ and use Eqs (4.2) and (4.11) to eliminate the velocity ratios (V_1/V_3) and (V_2/V_3). After simplification, this reduces to the important result

$$c_p^* = \frac{2x(y - 1)^2}{(y - x)} \tag{4.13}$$

Next consider a purely hypothetical reversible device which is not an ejector at all but a type of ideal turbomachine. This device receives two streams of fluid identical in all respects to the streams at stations 1 and 2 of the ideal ejector. It discharges a stream identical in all respects to the stream at station 3 of the ideal ejector except for the pressure p_{R3} which is higher than p_3^*. Again the density ρ is taken as constant. The reversible device operates adiabatically and hence isentropically. Under these conditions the following energy equation holds. Recall that $p_2 = p_1$.

$$x\dot{m}_3(p_1 + \tfrac{1}{2}\rho V_1^2) + (1 - x)\,\dot{m}_3\,(p_1 + \tfrac{1}{2}\rho V_2^2)$$

$$= \dot{m}_3\,(p_{3R} + \tfrac{1}{2}\rho V_3^2) \qquad (4.14)$$

The above equation can be simplified by subtracting from it, term by term, the following identity.

$$x\dot{m}_3 p_1 + (1 - x)\dot{m}_3 p_1 = \dot{m}_3 p_1 \qquad (4.15)$$

Upon carrying out the above subtraction, then dividing through by the reference power $\dot{m}_3\,(V_3^2/2)$ and simplifying, we readily find the pressure rise coefficient for the reversible device to be

$$\frac{(p_{3R} - p_3)}{\frac{1}{2}\rho V_3^2} = C_{PR} = \left\{ xy^2 + \frac{(1 - x)^3 y^2}{(y - x)^2} - 1 \right\} \qquad (4.16)$$

Comparison of this result with Eq. (4.13) shows that even the ideal ejector has a certain inherent mixing loss, call it c_m^*, as compared with a truly reversible device. Thus

$$c_m^* = (c_{PR} - c_p^*) \tag{4.17}$$

Of course the mixing loss c_m of the actual ejector will be somewhat larger than c_m^* and it is advantageous to express it in the form

$$c_m = \frac{c_m^*}{\eta_E} \tag{4.18}$$

where η_E, which we term ejector effectiveness, is a dimensionless parameter smaller than unity which must be determined from experimental data.

Eq. (4.18) identifies one of the component losses that reduce the actual pressure rise coefficient c_p below its ideal reversible value c_{PR}. Another loss is that associated with separation, friction and secondary flow effects within the ejector; let us denote it by symbol c_{fE}. We have seen that a third component is simply the gross electrical power output as expressed by the coefficient c_e. Thus the overall energy balance within the ejector requires that

$$c_p = c_{PR} - \frac{1}{\eta_E}(c_{PR} - c_p^*) - c_{fE} - c_e \tag{4.19}$$

The resulting pressure rise through the ejector as expressed by Eq. (4.19) must be just great enough to offset the losses in

the return passage. These again are losses associated with separation, friction and secondary flows; let us denote them by coefficient c_{fR}. Accordingly, for the return passage we may write

$$c_p = c_{fR} \tag{4.20}$$

We now eliminate c_p between Eqs. (4.19) and (4.20) and bring all terms to one side. We also introduce the following definition for the total friction loss in the fluid flywheel, namely,

$$c_f = c_{fE} + c_{fR} \tag{4.21}$$

The result is

$$c_{PR} - \left\{\frac{1}{\eta_E}\,(c_{PR} - c_p^*) + c_f\right\} - c_e = 0 \tag{4.22}$$

Now using Eqs. (4.13), (4.16) and (3.12) to express the above components in terms of variables x and y, we obtain

$$\left\{xy^2 + \frac{(1-x)^3y^2}{(y-x)^2} - 1\right\} - \left\{\frac{1}{\eta_E}\left[xy^2 + \frac{(1-x)^3y^2}{(y-x)^2} - 1 - \frac{2x(y-1)^2}{(y-x)}\right] + c_f\right\}$$
$$- \left\{\nu\,\frac{(1+5x)}{(1+2x)^2}\;xy^2\right\} = 0 \tag{4.23}$$

This is the overall energy balance equation for the "fluid flywheel" and it is fundamental. Notice that the term in the first pair of curly brackets represents the ideal power output of a reversible device, the term in the second pair of curly brackets represents the sum of the fluid power losses caused by mixing and friction and the term in the third pair of curly brackets represents the gross electrical power output.

Eq. (4.23) suggests the utility of defining a "conversion efficiency" η_{cv} as the ratio of the gross electrical power c_e to the ideal power c_{PR}. Thus

$$\eta_{cv} = \frac{c_e}{c_{PR}} = \frac{\left\{ \nu \frac{(1 + 5x)}{(1 + 2x)^2} \, xy^2 \right\}}{\left\{ xy^2 + \frac{(1 - x)^3 y^2}{(y - x)^2} - 1 \right\}} \tag{4.24}$$

Notice that low values of the parameter ν, which is ultimately determined by the electrical breakdown limit, will necessarily produce low conversion efficiencies.

In connection with Eq. (4.23) and (4.24), notice that x always falls between zero and unity while y is always greater than unity but has no preassigned upper limit.

Assuming that parameters η_E, c_f and ν are known or can be estimated, Eq. (4.23) then fixes a corresponding unique relation between variables x and y. This may be described by a line in the xy plane. All subsequent calculations must be confined to points that lie along this line.

If the area ratio $\frac{A_1}{A_3}$ be already fixed, then we have from Eq. (4.8) the additional constraint

$$\left(\frac{A_1}{A_3}\right) = \left(\frac{x}{y}\right) \tag{4.25}$$

Of course for a fixed value of (A_1/A_3), Eq. (4.25) also represents a line in the xy plane. In fact it is a straight

line of slope (A_3/A_1) which passes through the origin. The one or more points of intersection of this straight line with the curve associated with Eq (4.23) fix the conditions at which steady operation of the fluid flywheel is possible. The location of such a point determines the values of x and y and hence ultimately determines all other performance characteristics of the system as well.

Notice that Eq. (4.23) lends itself to further algebraic simplification which makes the subsequent numerical solution easier. On the other hand the terms in the simplified result cannot be given the clear physical interpretation that is possible with Eq. (4.23) itself. After simplification, Eq. (4.23) becomes

$$\frac{1}{\eta_E} \cdot \frac{2x(y-1)^2}{(y-x)} - \left(\frac{1}{\eta_E} - 1\right)\left\{xy^2 + \frac{(1-x)^3 y^2}{(y-x)^2} - 1\right\}$$

$$- \nu \frac{(1+5x)}{(1+2x)^2} xy^2 - c_f = 0 \qquad (4.26)$$

For purposes of numerical solution, it is useful to cast Eq. (4.26) into a more tractable form as follows. Let

$$A_1 = \frac{2(y-1)^2}{\eta_E} \qquad (4.27)$$

$$A_2 = \left(\frac{1}{\eta_E} - 1\right) y^2 \qquad (4.28)$$

$$A_3 = \nu y^2 \qquad (4.29)$$

$$A_4 = c_f - \frac{1}{\eta_E} + 1 \tag{4.30}$$

With this notation, Eq. (4.26) may be rewritten as follows, where F is a function that must equal zero. Thus

$$F = A_1 \frac{x}{(y-x)} - A_2 \left[x + \frac{(1-x)^3}{(y-x)^2} \right] - A_3 \frac{(1+5x)x}{(1+2x)^2} - A_4 = 0 \tag{4.31}$$

Next we multiply through by $(1 + 2x)^2 (y - x)^2$ and denote the resulting function by G. Upon expanding the right side, regrouping terms and simplifying, we find that G is a quartic in x. The coefficients of this polynomial turn out to be

$$B_4 = -4A_1 - 4(3-2y)A_2 - 5A_3 - 4A_4 \tag{4.32}$$

$$B_3 = 4(y-1)A_1 - 4y(y-2)A_2 + (10y-1)A_3 + 4(2y-1)A_4 \tag{4.33}$$

$$B_2 = (4y-1)A_1 - (4y^2-2y-5)A_2 - y(5y-2)A_3 - (4y^2-8y+1)A_4 \tag{4.34}$$

$$B_1 = yA_1 - (y^2+1)A_2 - y^2A_3 - 2y(2y-1)A_4 \tag{4.35}$$

$$B_0 = -A_2 - y^2A_4 \tag{4.36}$$

The function G may then be written

$$G = B_4x^4 + B_3x^3 + B_2x^2 + B_1x + B_0 = 0 \tag{4.37}$$

The unknown root x can be found by Newton's method. For this purpose we require also the derivative of G which is

$$G' = 4B_4x^3 + 3B_3x^2 + 2B_2x + B_1 \tag{4.38}$$

Let x_n be any trial value of x and let G_n and G'_n be the corresponding values computed from Eqs. (4.37) and (4.38). Then according to Newton's method, the next trial value x_{n+1} should be taken as

$$x_{n+1} = x_n - \frac{G_n}{G'_n} \tag{4.39}$$

This procedure converges rapidly to the true root x. This method was used in calculating the numerical example which is presented in a later section.

5. Thermodynamic Performance

As shown in the schematic temperature entropy diagram, Fig 5:1, the fluid flywheel receives a supply $\dot{m}_1$ (kg/sec) of superheated steam at condition p_o , T_o and discharges saturated or nearly saturated liquid at condition p_4 , T_4 . It gives up heat to the ambient atmosphere at absolute temperature T_A and delivers a gross electrical power output P_e (watts). It also requires an input of electric power, call it P_x , to energize the injector. This is normally a small percentage of the gross electrical output and is conveniently expressed by means of an excitation efficiency η_x such that

$$\left(P_e - P_x\right) = P'_e = \eta_x P_e \qquad \text{(watts)} \qquad (5.1)$$

(continued on page 5-3)

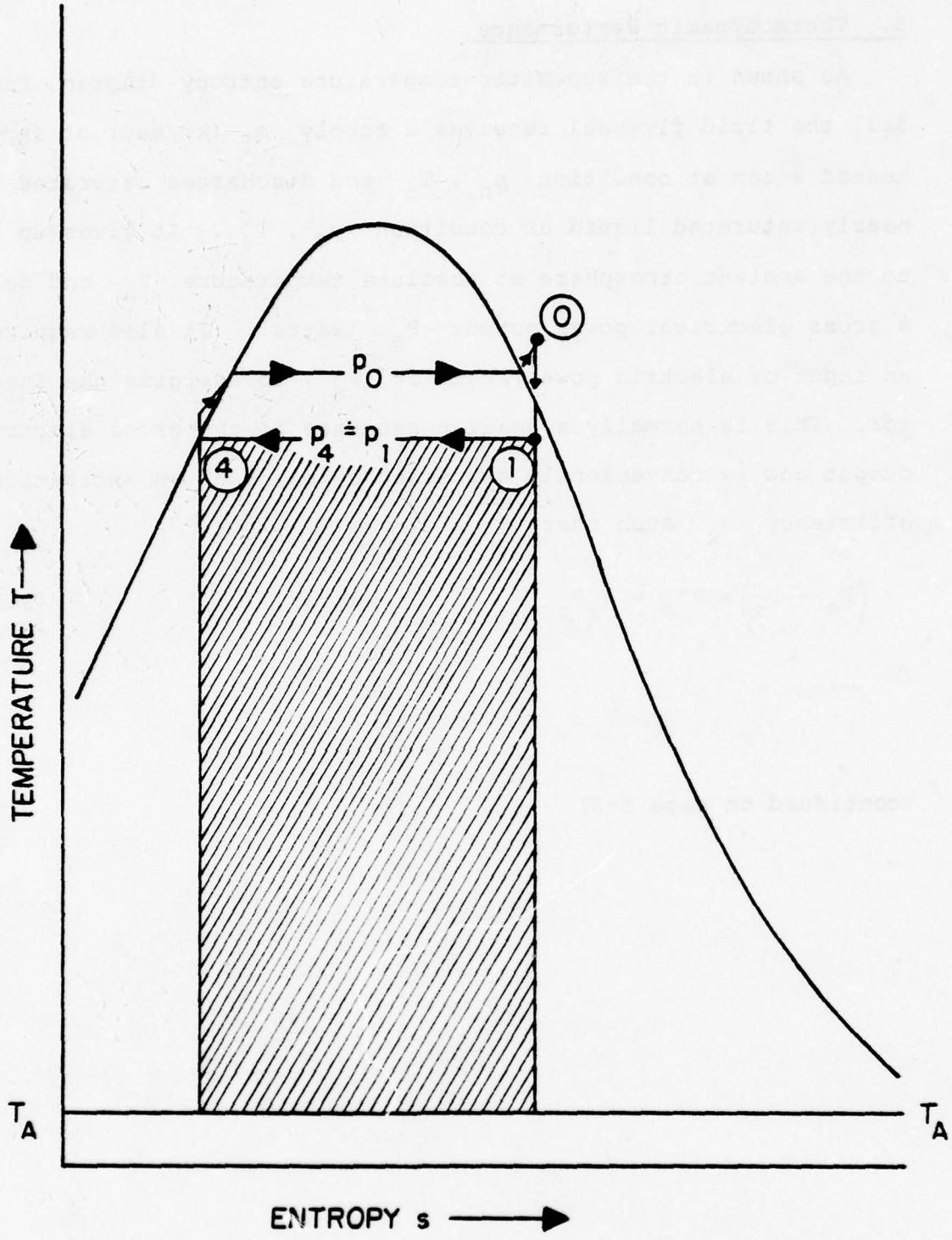

Fig. 5.2. Schematic Temperature Entropy Diagram for Primary Stream.

After being condensed and leaving the fluid flywheel, the liquid water must be pumped back into the boiler. For an ideal pump of 100% efficiency this would require the expenditure of shaft power in the amount

$$P_p^* = \dot{m}_1 (p_o - p_4) v_4 \quad \text{(watts)} \qquad (5.2)$$

where v_4 denotes the specific volume of the liquid at state 4.

For a real pump of efficiency η_p the corresponding power is

$$P_p = \frac{P_p^*}{\eta_p} \quad \text{(watts)} \qquad (5.3)$$

Thus it is seen that for the overall cycle, the net useful power output may be written as

$$P_e'' = (\eta_x P_e - P_p^*/\eta_p) \quad \text{(watts)} \qquad (5.4)$$

The rate of heat input to the steam passing through the boiler and superheater is

$$\dot{Q} = \dot{m}_1 (h_o - h_4) - P_p^*/\eta_p \quad \text{(watts)} \qquad (5.5)$$

where h_o and h_4 denote the enthalpies (joule/kg) at states o and 4.

For the hypothetical case of 100% pump efficiency, we denote the corresponding heat rate calculated from Eq. (5.5) by symbol $\dot{Q}^*$. This differs only very slightly from $\dot{Q}$.

The overall cycle efficiency now becomes

$$\eta_c = \frac{P_e''}{\dot{Q}} = \frac{1}{\dot{Q}}\left(\eta_x P_e - P_p^*/\eta_p\right) \tag{5.6}$$

It is of interest to compare the above performance of the actual EGD device with the ideal performance of a hypothetical reversible device operating under the same input, output and ambient conditions. According to the theory of availability in steady flow, the maximum electrical power that could be produced by such an ideal device is

$$P_e^* = \dot{m}_1 \left\{(h_o - h_4) - T_A\,(s_o - s_4)\right\} \quad \text{(watts)} \tag{5.7}$$

where s_o and s_4 denote the entropies at states o and 4, respectively (joule/kg ^oK).

The cycle efficiency of this ideal device would be

$$\eta_c^* = \frac{1}{\dot{Q}^*}\,(P_e^* - P_p^*) \tag{5.8}$$

It is also instructive to compare the net output of the real system with that of the above ideal and reversible device. We term this ratio the relative output. Thus

$$\eta_{rel} = \left(\frac{\eta_x P_e - P_p^*/\eta_p}{P_e^* - P_p^*}\right) \tag{5.9}$$

All of the foregoing relations can be put into dimensionless form by dividing all quantities having the units of power by a suitable reference power. In the previous analysis of the fluid

flywheel, it was natural and convenient to choose this reference as the kinetic power of the total stream at the ejector exit, station 3. While it would be possible to retain this same reference in this section, it is advantageous to choose here as reference, the kinetic power of the primary jet at the ejector inlet, station 1. This choice reduces the final results to a simpler form and makes them somewhat easier to interpret. Thus the reference power is now

$$\dot{m}_1\left(\frac{V_1^2}{2}\right) = \dot{m}_1\ (h_o - h_1) \tag{5.10}$$

In computing this reference power it is permissible to assume that state 1 is fixed by the two conditions

$$s_1 = s_o \tag{5.11}$$

$$p_1 = p_4 \tag{5.12}$$

In connection with Eq. (5.10) it is also instructive to note that

$$(h_o - h_1) = \frac{V_1^2}{2} = \frac{\frac{1}{2}\, a_o^2 M_1^2}{\left[1 + \frac{\gamma-1}{2} M_1^2\right]} \tag{5.13}$$

Recall also that if we introduce the optimizing condition developed earlier, namely,

$$M_1^2 = M_{1opt}^2 = \frac{1}{2} \tag{5.14}$$

then Eq (5.13) simplifies further to

$$(h_o - h_1) = \frac{V_1^2}{2} = \frac{a_o^2}{(\gamma+3)} \tag{5.15}$$

Incidentally, it is also worth noting that the overall pressure ratio across the fluid flywheel is

$$\left(\frac{p_4}{p_o}\right) \doteq \left(\frac{p_1}{p_o}\right) = \left[1 + \left(\frac{\gamma-1}{2}\right) M_1^2\right]^{-\left(\frac{\gamma}{\gamma-1}\right)} \tag{5.16}$$

Moreover, if we observe the restriction of Eq (5.16) this becomes

$$\left(\frac{p_4}{p_o}\right) \doteq \left(\frac{p_1}{p_o}\right) = \left[\frac{4}{\gamma+3}\right]^{\left(\frac{\gamma}{\gamma-1}\right)} \tag{5.17}$$

For example, for $\gamma = 1.3$ this gives

$$\left(\frac{p_4}{p_o}\right) \doteq \left(\frac{p_4}{p_o}\right) = 0.731 \tag{5.18}$$

This result expresses one of the fundamental limitations of the fluid flywheel concept, namely the restriction to a fixed pressure ratio. The reason for this restriction was explained earlier in connection with Fig. 2.1.

Upon simplifying and reducing the various foregoing thermodynamic relations in the manner explained above, we obtain the following results.

$$\frac{P_e^*}{\dot{m}_1(h_o-h_1)} = K_e^* = \left\{1 + \frac{(T_4-T_A)(s_o-s_4)}{(h_o-h_1)}\right\} \quad \text{Reversible Electric Power} \quad (5.19)$$

$$\frac{P_p^*}{\dot{m}_1(h_o-h_1)} = K_p^* = \left\{\frac{(p_o-p_4)v_4}{(h_o-h_1)}\right\} \quad \text{Reversible Pump Power} \quad (5.20)$$

$$\frac{\dot{Q}^*}{\dot{m}_1(h_o-h_1)} = K_Q^* = \left\{\frac{(h_o-h_4)}{(h_o-h_1)} - K_p^*\right\} \quad \text{Reversible Heat Input} \quad (5.21)$$

$$\frac{\dot{Q}}{\dot{m}_1(h_o-h_1)} = K_Q = \left\{\frac{(h_o-h_4)}{(h_o-h_1)} - \frac{K_p^*}{\eta_p}\right\} \quad \text{Actual Heat Input} \quad (5.22)$$

$$\frac{P_e}{\dot{m}_1(h_o-h_1)} = K_e = \nu\,\frac{(1+5x)}{(1+2x)^2} \quad \text{Gross Electric Power} \quad (5.23)$$

$$\frac{P_e''}{\dot{m}_1(h_o-h_1)} = K_e'' = \left(\eta_x K_e - \frac{K_p^*}{\eta_p}\right) \quad \text{Net Electric Power} \quad (5.24)$$

$$\eta_c = \frac{1}{K_Q}\left(\eta_x K_e - \frac{K_p^*}{\eta_p}\right) \quad \text{Cycle Efficiency} \quad (5.25)$$

$$\eta_c^* = \frac{1}{K_Q^*}\,(K_e^* - K_p^*) \quad \text{Reversible Cycle Efficiency} \quad (5.26)$$

$$\eta_{rel} = \left\{\frac{\eta_x K_e - K_p^*/\eta_p}{K_e^* - K_p^*}\right\} \quad \text{Relative Output} \quad (5.27)$$

Once Eq. (4.37) of the previous section is solved, it becomes a relatively straight forward matter to apply the relations of the present section to calculate the various thermodynamic performance parameters. Recall that Eq. (4.37) defines a whole series of points in the xy plane. By calculating the thermodynamic performance parameters of this section for such a series of points, and by comparing the respective results, it becomes possible to choose that optimum design point which yields the best overall trade off among the various desired performance characteristics.

So far only an initial trial calculation of this type has been made on the basis of a plausible initial set of key parameters. This result is summarized in a later section.

6. Summary of Principal Calculation Formulas

The principal equations developed in the preceding sections are summarized below for easy reference. They are listed without further explanation in the approximate order in which they would be used in a typical calculation.

Input Parameters

$$\alpha = \left(\frac{C_o}{C_B}\right)\left(\frac{T_o}{p_o}\right)\left[\frac{\gamma+3}{4}\right]^{\frac{1}{(\gamma-1)}} \tag{6.1}$$

$$\beta = \left(\frac{\varepsilon C_B{}^2 p_o}{T_o{}^2}\right) \tag{6.2}$$

$$\psi = \frac{3}{\gamma}\left[\frac{4}{\gamma+3}\right]^{\left(\frac{\gamma+1}{\gamma-1}\right)} (1+\alpha)^2 \tag{6.3}$$

$$\nu = \mu\psi\beta \tag{6.4}$$

$$\frac{V_1{}^2}{2} = (h_o - h_1) \quad (\text{where } s_1 \doteq s_o,\ p_1 \doteq p_4) \tag{6.5}$$

$$K_e{}^* = \left\{1 + \frac{(T_4 - T_A)(s_o - s_4)}{(h_o - h_1)}\right\} \tag{6.6}$$

$$K_p{}^* = \left\{\frac{(p_o - p_4)v_4}{(h_o - h_1)}\right\} \tag{6.7}$$

$$K_Q{}^* = \left\{\frac{(h_o - h_4)}{(h_o - h_1)} - K_p{}^*\right\} \tag{6.8}$$

$$K_Q = \left\{ \frac{(h_o - h_4)}{(h_o - h_1)} - \frac{K_p^*}{\eta_p} \right\} \tag{6.9}$$

$$\eta_c^* = \frac{1}{K_Q^*} \left(K_e^* - K_p^* \right) \tag{6.10}$$

Solution of Energy Balance Equation

$$A_1 = \frac{2(y-1)^2}{\eta_E} \tag{6.11}$$

$$A_2 = \left(\frac{1}{\eta_E} - 1 \right) y^2 \tag{6.12}$$

$$A_3 = \nu y^2 \tag{6.13}$$

$$A_4 = \left(c_f - \frac{1}{\eta_E} + 1 \right) \tag{6.14}$$

$$B_4 = -4A_1 - 4(3-2y)A_2 - 5A_3 - 4A_4 \tag{6.15}$$

$$B_3 = 4(y-1)A_1 - 4y(y-2)A_2 + (10y-1)A_3 + 4(2y-1)A_4 \tag{6.16}$$

$$B_2 = (4y-1)A_1 - (4y^2-2y-5)A_2 - y(5y-2)A_3 - (4y^2-8y+1)A_4 \tag{6.17}$$

$$B_1 = yA_1 - (y^2+1)A_2 - y^2A_3 - 2y(2y-1)A_4 \tag{6.18}$$

$$B_o = -A_2 - y^2A_4 \tag{6.19}$$

$$G = B_4x^4 + B_3x^3 + B_2x^2 + B_1x + B_o \tag{6.20}$$

$$G' = 4B_4x^3 + 3B_3x^2 + 2B_2x + B_1 \tag{6.21}$$

$$x_{n+1} = x_n - \frac{G_n}{G_n'}, \qquad \text{(Iterate until } x \text{ converges)} \tag{6.22}$$

Output Parameters

$$K_e'' = \left\{ \eta_x \nu \frac{(1+5x)}{(1+2x)^2} - \frac{K_p^*}{\eta_p} \right\} \qquad \text{Net Electric Power} \qquad (6.23)$$

$$\eta_c = \frac{K_e''}{K_Q} \qquad \text{Cycle Efficiency} \qquad (6.24)$$

$$\eta_{rel} = \frac{K_e''}{(K_e^* - K_p^*)} \qquad \text{Relative Output} \qquad (6.25)$$

$$K_e = \left\{ \nu \frac{(1+5x)}{(1+2x)^2} \right\} \qquad \text{Gross Electric Power} \qquad (6.26)$$

$$K_{PR} = \left\{ 1 + \frac{(1-x)^3}{x(y-x)^2} - \frac{1}{xy^2} \right\} \qquad \text{Ideal Pressure Rise} \qquad (6.27)$$

$$\eta_{cv} = \frac{K_e}{K_{PR}} \qquad \text{Conversion Efficiency} \qquad (6.28)$$

Note: Power coefficients denoted by symbol K are expressed in terms of the kinetic power at station 1. Those denoted by symbol c are expressed in terms of the kinetic power at station 3. The conversion between these two forms is simply

$$K = \frac{c}{xy^2} \qquad (6.29)$$

7. Some Typical Experimental Data and Preliminary Numerical Results

Reference (1) reports measurements of breakdown field strength as a function of pressure at constant temperature and electrode separation. Their results show that $C_o = 9 \times 10^5$ v/m and $C_B = 9.5 \times 10^3$ m^2 $^oK/C$. Note the interesting fact that steam and air appear to have identical breakdown properties!

A system now under development by Marks Polarized Corporation is intended to operate with steam at about 100 atmospheres pressure and sufficient superheat to give about 5% moisture at state 1. The data in Table 7.1 suggest that under these conditions, approximately, from Eqs. (6.1) and (6.2),

$$\alpha = \left(\frac{C_o}{C_B}\right)\left(\frac{T_o}{P_o}\right)\left[\frac{\gamma+3}{4}\right]^{\frac{1}{(\gamma-1)}}$$

$$= \frac{\left[0.920 \times 10^6\right]\left[591\right]\left[1.273\right]}{\left[0.953 \times 10^4\right]\left[10.34 \times 10^6\right]} = 0.0070 \approx 0 \qquad (7.1)$$

$$\beta = \left(\frac{\varepsilon C_B{}^2 P_o}{T_o{}^2}\right) = \frac{\left[8.85 \times 10^{-12}\right]\left[0.953 \times 10^4\right]^2\left[10.34 \times 10^6\right]}{\left[591\right]^2}$$

$$= 0.0238 \qquad (7.2)$$

Then from Eq. (6.3) we obtain

$$\psi = \frac{3}{\gamma}\left[\frac{4}{\gamma+3}\right]^{\left(\frac{\gamma+1}{\gamma-1}\right)}(1+\alpha)^2 = \frac{3}{1.3}\left[\frac{4}{4.3}\right]^{\left(\frac{2.3}{0.3}\right)}(1+0)^2 \qquad (7.3)$$

$$= 1.32$$

In the absence of adequate test date, the best estimate of μ that is possible at this time is simply

$$\mu \approx 1 \qquad (7.4)$$

According to Eq. (6.4) this gives the estimate

$$\nu = \mu\psi\beta = (1)(1.32)(0.0238) = 0.032 \qquad (7.5)$$

The value of the flow loss factor c_f for the annulus may be estimated from the data in Ref. (2) on losses in pipe bends. At a Reynolds number of 200,000 or above, these losses are mainly a function of R/r, where R is bend radius and r is pipe radius. For the torus in Marks' design $R/r = 5.7$. Ref. (2) shows that at this value of R/r the loss factor for a 180° pipe bend is about 0.4. Thus for a 360° turn the loss factor would presumably be twice the value or approximately

$$c_f \approx 0.8 \qquad (7.6)$$

There are qualitative grounds for hoping that the loss in a true torus might be somewhat smaller than the above pipe bend data would suggest, but there is no hard data available on this point. Thus Eq. (7.6) represents a plausible and conservative

working hypothesis that can be advanced at this time.

Values of η_E can be estimated from available test data on ejector performance. See, for example, Ref. (3). These data have not yet been reviewed critically. All we can say at present on the basis of general engineering judgment and experience is that for the range of ejector design parameters of interest in the present context, η_E is unlikely to lie above 0.9 or below 0.5. It is thought reasonable as a tentative initial working hypothesis to choose

$$\eta_E \approx 0.8 \tag{7.7}$$

Also required for the calculation are certain thermodynamic properties. These are summarized in Table 7.1. These data happen to be in English units but this is permissible because the final results, being dimensionless, are independent of the system of units used. For some purposes the steam was treated approximately as a perfect gas with a ratio of specific heats $\gamma = 1.3$.

The information in Table 7.1, along with the formulas of Section 6, permit the various key input parameters to be estimated as summarized in Table 7.2. These values are regarded as the best estimates that are possible at the present time. These input data suffice to permit a corresponding performance calculation to be carried out. This has been done and the main results are summarized in Table 7.3 and in Fig. 7.1. Notice that each row or Table 7.3 corresponds to a different value of the ejector area ratio A_1/A_3.

Table 7.1 Thermodynamic Properties

State		0	1	4	Ambient
p	psia	1500	1100	1100	--
T	^{o}R	1063.9	1016	1016	530
h	Btu/lbm	1180.7	1156.3	557.4	--
s	Btu/lbm^{o}R	1.3470	1.3470	0.7575	--
ρ	lbm/ft^3	--	--	45.45	--

Table 7.2 Estimated Values of Key Input Parameters

$\gamma = 1.3$	$\eta_p = 0.9$
$\mu = 1$	$K_e^* = 12.7$
$\nu = 0.032$	$K_p^* = 0.067$
$\eta_E = 0.8$	$K_Q^* = 25.5$
$c_f = 0.8$	$K_Q = 25.5$
$\eta_x = 1$	$\eta_c^* = 0.50$

Table 7.3 Estimated Performance of EHD Generator

y	x	A_1/A_3	K_{PR}	η_{cv}	K_e''	η_{rel}	η_c
1.6000	0.9093	0.5683	0.5722	0.0390	-0.0521	-0.0041	-0.0020
1.8000	0.7932	0.4407	0.6219	0.0382	-0.0507	-0.0040	-0.0020
2.0000	0.6950	0.3475	0.6642	0.0377	-0.0494	-0.0039	-0.0019
2.2000	0.6164	0.2802	0.7013	0.0374	-0.0482	-0.0038	-0.0019
2.4000	0.5546	0.2311	0.7338	0.0370	-0.0473	-0.0037	-0.0019
2.6000	0.5062	0.1947	0.7620	0.0366	-0.0465	-0.0037	-0.0018
2.8000	0.4683	0.1672	0.7867	0.0362	-0.0459	-0.0036	-0.0018
3.0000	0.4385	0.1462	0.8081	0.0359	-0.0454	-0.0036	-0.0018
3.2000	0.4151	0.1297	0.8269	0.0355	-0.0451	-0.0036	-0.0018
3.4000	0.3970	0.1168	0.8433	0.0352	-0.0448	-0.0035	-0.0018
3.6000	0.3833	0.1065	0.8578	0.0349	-0.0445	-0.0035	-0.0017
3.8000	0.3734	0.0983	0.8706	0.0345	-0.0444	-0.0035	-0.0017
4.0000	0.3667	0.0917	0.8820	0.0342	-0.0443	-0.0035	-0.0017
4.2000	0.3630	0.0864	0.8922	0.0339	-0.0442	-0.0035	-0.0017
4.4000	0.3621	0.0823	0.9013	0.0336	-0.0442	-0.0035	-0.0017
4.6000	0.3640	0.0791	0.9096	0.0332	-0.0442	-0.0035	-0.0017
4.8000	0.3687	0.0768	0.9170	0.0329	-0.0445	-0.0035	-0.0017
5.0000	0.3762	0.0752	0.9239	0.0325	-0.0444	-0.0035	-0.0017
5.2000	0.3869	0.0744	0.9301	0.0321	-0.0446	-0.0035	-0.0017
5.4000	0.4009	0.0742	0.9359	0.0316	-0.0448	-0.0035	-0.0018

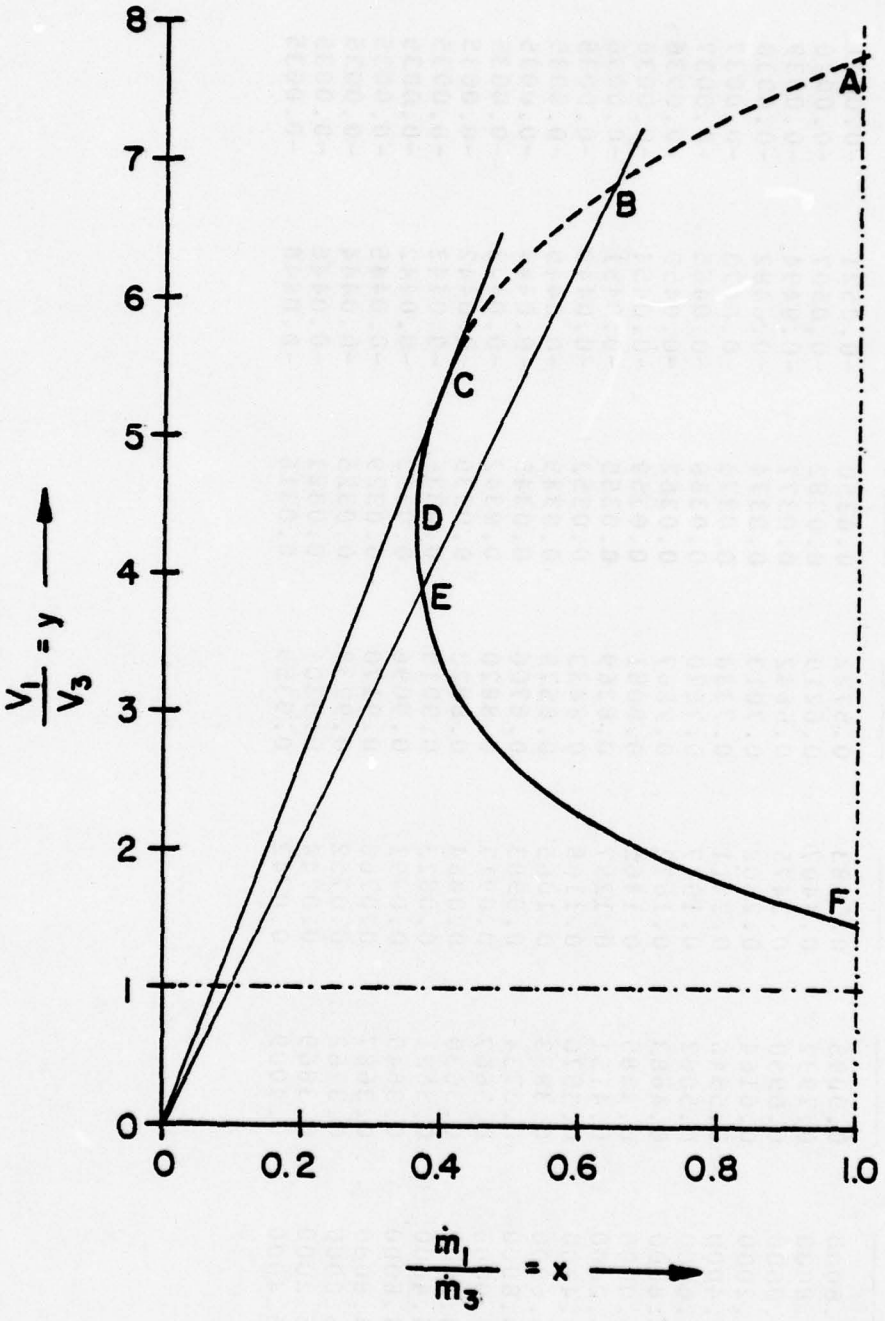

Fig. 7.1 Results of Energy Balance

The curve ABCDEF shown in Fig. 7.1 is the locus of points x,y which satisty the basic energy balance relation of the ejector and fluid flywheel, that is, Eq. (4.23). In view of the tentative nature of the values assigned to parameters ν, η_E and c_f, the accuracy of this curve is somewhat uncertain, but its general qualitative features are undoubtedly correct. Any straight line through the origin, such as line OEB, for example, represents Eq. (4.25), and the inverse of its slope represents the area ratio A_1/A_3. Notice that such a straight line may in general intersect the curve at two points such as E and B, for example. It can be shown that only the lower point E represents stable equilibrium; point B represents unstable equilibrium and should be disregarded. For this reason the entire dashed portion ABC of the curve must also be discarded. Only the solid portion CDEF has any practical significance.

Notice that the tangent point C represents the lowest value of A_1/A_3 and the highest value of y that can be achieved in steady state operation. Recall that the gross electric power is proportional to the factor $(1+5x)/(1+2x)^2$. It can be shown that this factor reaches its peak value of 1.04 at $x = 0.1$. It is therefore desirable to choose the operating point on the curve as close to $x = 0.1$ as possible. In this case the nearest point is at D where $x = 0.36$. Note that this is the lowest value of x that can be attained for the assumed values of ν, η_E and c_f.

The corresponding value of the factor $(1+5x)/(1+2x)^2$ is 0.95.

Notice from the data in Table 7.2 that an ideal reversible device operating on the given basic thermodynamic cycle would produce a dimensionless net power output of amount

$$(K_e^* - K_p^*) = 12.7 - 0.07 \approx 12.6 \tag{7.8}$$

and would produce an ideal cycle efficiency of amount

$$\eta_c^* = 0.50 \tag{7.9}$$

These theoretical performance limits of the ideal reversible device are in themselves very favorable. Unfortunately, the performance of the actual EHD system as summarized in Table 7.3 is seen to be very unsatisfactory. In fact the net power outputs and cycle efficiencies are <u>negative</u> for all possible operating points! This means that even at 100 atmospheres pressure, the phenomenon of electrical breakdown so severely limits the gross electrical power output that it it insufficient even to meet the demand for power to drive the pump, let alone provide any useful output.

It might be supposed that a radical increase in the electrical breakdown strength, if it could be achieved, would in itself transform this pessimistic picture into an optimistic one, but this is not entirely the case, at least not for the present EHD scheme. Suppose for example, that the breakdown parameter ν could be increased by a factor of roughly 30 so as to bring the gross electrical power coefficient up say to

$$K_e \approx 1 \tag{7.10}$$

In that case the cycle efficiency would still be only about

$$\eta_c = \frac{1}{K_Q}\left(\eta_x K_e - \frac{K_p^*}{\eta_p}\right) \approx \frac{1}{25.5}\ (1 - 0.07) \approx 0.037 \qquad (7.11)$$

or less than 4%. The main reason for this unsatisfactory result is that the present cycle squanders available energy by dumping heat from the condenser at high temperature to the ambient air at low temperature without extracting any useful power from it. The irreversibilities inherent in the ejector also waste available energy. Moreover, friction losses in the fluid flywheel appear to be disappointingly high. As a reflection of these losses, note from Table 7.3 that the conversion efficiency η_{cv} remains below 4% for all possible stable operating points.

It is also worthwhile at this point to review the various factors that affect the important parameter ν which so severely limits the electrical output. These factors are revealed clearly in Eqs. (6.2), (6.3) and (6.4). It is convenient to combine them here in the following way, assuming $\alpha \simeq 0$. Thus

$$\nu = \mu\left\{\frac{3}{\gamma}\left[\frac{4}{\gamma+3}\right]^{\frac{\gamma+1}{\gamma-1}}\right\}\left(\frac{\varepsilon C_B^{\,2} p_0}{T_0^{\,2}}\right) \qquad (7.12)$$

As γ varies from 1 to 1.67, the function of γ in the curly brackets above varies from 1.82 to 0.97. Hence there is no possibility of radically changing the order of magnitude of ν by manipulating γ.

Similar considerations apply to the quantity ε. It has been suggested, see Re. 4, that ε might be increased by using a polarizable aerosol. But the overall increase that can be achieved in this way is expected to be less than a factor of ten and, as we have seen, this in itself is not enough to overcome fully the limitations of the present EHD scheme.

An obvious way to increase ν is to increase p_o. We have noted, however, that even at 100 atmospheres pressure, ν is still much too small. Any increase beyond this value is not feasible for two reasons. Firstly, structural and practical problems become troublesome at such high pressures. Secondly the linear relation between electrical breakdown strength and fluid density as given by Eq. (2.5) breaks down near pressures of 100 atmospheres. See Ref. 1.

The two remaining factors at our disposal are C_B and T_o. Note that ν is proportional to the quadractic factor $(C_B/T_o)^2$. The breakdown constant C_B is a property of the medium. The question whether any aerosol mixture exists that has a substantially higher value of C_B has not been investigated. It is recommended that such an investigation be carried out.

Finally consider the factor T_o. In the present scheme, charged particles of low mobility are created by condensation. This requires that T_o be high enough to produce about 5% liquid at state 1. This restriction on T_o could be eliminated by abandoning the condensation method and utilizing instead the

direct injection of liquid droplets or solid particles. This change also entails changing the carrier fluid from steam to air or some other noncondensing gas. Note that a decrease in T_o from 1016 ^oR to 530 ^oR would increase ν by a factor of about 3.7.

It seems possible that some combination of the above methods could perhaps increase ν by a factor of say 20 or so. We have seen that this in itself would not make the present fluid flywheel configuration successful. Nevertheless, an improvement of this order might very well suffice to make some alternative EHD scheme practical.

8. Conclusions and Recommendations.

Broadly speaking, one of the inherent limitations of EHD power generation is the severe restriction imposed by the phenomenon of electrical breakdown. Because of this effect, the electrical work that can be extracted per unit mass of working fluid is very small. In general there are two distinct approaches for attempting to overcome this limitation. One method is based on multi-staging, that is, on passing the same working fluid through a whole series of successive electrical conversion sections. The other method is to adopt an ejector system which utilizes a primary stream of high velocity but low mass flow rate to drive a secondary stream of low velocity but high mass flow rate. The conversion of flow energy to electric work is accomplished in the resulting low velocity stream. Although electrical work per unit mass of low velocity fluid remains low, the electrical work per unit mass of high velocity primary fluid may be boosted to a sufficiently high value. The effectiveness of this scheme is limited to some extent by the characteristic ejector mixing losses.

In this report, a proposed type of single stage EHD generator is analyzed which utilized the ejector principle. However, this design combines the ejector and the electrical conversion section into a single unit; in particular, charged particles are introduced into the primary stream only and are subsequently collected at the ejector exit section.

The analysis shows that, unfortunately, this type of design gives extremely poor performance. In fact the electrical power

generated is insufficient to drive the feedwater pump, let alone produce any net useful output. This poor result can be attributed to the fact that the charged particles are introduced into the primary stream, thus generating a very intense local electrical field at this point.

An obvious remedy for this difficulty is to place the electrical conversion section after the ejector where the electrical field can be much lower. The Appendix evaluates this revised design. It is shown in the Appendix that under the most optimistic assumptions, the cycle efficiency is less than 4% which may be insufficient to compete with alternative power systems.

It may be possible to multi-stage the fluid flywheel generators and thereby show an order of magnitude improvement in performance. It is recommended that systematic parametric studies be carried out to determine the performance possibilities of such a multi-stage system and to estimate optimum design values of the key parameters. It would also be advisable in the interest of orderly development to restrict this proposed next step to the same basic medium, namely steam, and to the same basic Rankine cycle as used in the previous studies. Of course there is no assurance that a multi-stage design will necessarily prove successful because, even if the theoretical cycle performance is favorable, practical considerations of bulk and complexity might nullify the theoretical advantages.

9. References

* Alvin Marks of the Marks Polarized Corporation. See "Conversion of Heat to Electrical Power by Means of a Charged Aerosol", Final Report on Contract NOw 63-0225-C, Marks Polarized Corp. to Bureau of Naval Weapons, Washington, D.C. (Dec 30, 1963) AS 429304.

1. N.M. Huberman, H. Shelton, W. Krieve, and C.L. Dailey, "Study of Electrofluid Dynamic Power Conversion", Report No. AFAPL-TR-76-31 (July 1976). Also, Lawson, M.O., Fretter, E.F., and Griffith, R.W., "Report on Progress in Achieving Direct Energy Conversion of a Major Fraction of Sonic Flow Kinetic Power into Electric Power by Electrofluid Dynamic (EFD) Process", 9th Intersociety Energy Conversion Engineering Conference, San Francisco, CA, (Aug 26-30, 1974).

2. H. Itō, "Pressure Losses in Smooth Pipe Bends", Trans. ASME (D), Journ. of Basic Engr, 82, No. 1, 131 (1960).

3. S.H. Hasinger, "Performance Characteristics of Ejector Devices", ARLTR 75-0205 (June 1975); "Comparison of Experiment and Analysis for a High Primary Mach Number Ejector", AFFDL-TR-38 (May 1977); "Ejector Optimization", AFFDL-TR-23 (June 1978).

4. Marks, A.M., "Optimum Charged Aerosols for Power Conversion", JAP, 43, 219 (1972).

APPENDIX: Performance Characteristics of Revised EHD Generator

The analysis in the main text clearly indicates that introducing charges in the primary stream only, limits the thermodynamic state 1 to a relatively high fixed pressure ratio (p_1/p_o = 0.731 for M_1 = 0.71). An obvious improvement is to uncouple the ejector from the electrical conversion section. This is done in the following analysis in which the electrical conversion section is located after the ejector.

The work in this Appendix is based on a fixed upper pressure p_o = 1500 psia and a fixed steam quality of 0.950 at station 1 (See Fig. 5.1). However, the back pressure p_1 is allowed to take on a large number of possible values ranging from 1400 psia down to 14.7 psia. At any given back pressure, the area ratio A_3/A_1 is allowed to vary as required to obtain best performance. It is found that best performance corresponds to the minimum possible value of the mass flow ratio ($\dot{m}_1/\dot{m}_3$) = x. This is governed by the energy balance equation for the fluid flywheel.

Three cases are considered, as listed in more detail on page 2A. Case A represents the present best estimate of the three key parameters $\eta_{/R}$, c_f and C_B. Case B represents a much more optimistic estimate of parameters η_R and c_f, perhaps values which can never be achieved practically. Case C retains these optimistic values of η_R and c_f and assumes in addition that the electrical breakdown constant C_B can be increased by a factor of $\sqrt{10}$. Thus, case C represents optimism plus a fundamental

REVISED EHD ANALYSIS

BASIS

* Design change: electrical power section now placed <u>after</u> ejector.
* Rankine cycle with -

  p_o = 1500 psia

  steam quality at state 1 = 0.95

OPTIMIZING PARAMETERS

* Pressure p_1 in fluid flywheel
* Ejector area ratio A_1/A_3

CASES STUDIED

		A	B	C
Ejector Effectiveness	η_E	0.8	0.9	0.9
Friction Factor	c_f	0.8	0.1	0.1
Electrical Breakdown Constant (m^2 °K/Coulomb)	C_B	9.49×10^3	9.49×10^3	$\sqrt{10} \times 9.49 \times 10^3$

scientific "break-through".

The single most important result of the analysis is the curve of cycle efficiency η_c versus back pressure p_1, Fig. 1. This result confirms that the proposed design revision has indeed improved the performance over that of the original version. Recall that the original design yielded a negative cycle efficiency! The revised design, case A, produces positive efficiencies for values of p_1 above about 900 psia. The peak efficiency occurs approximately at p_1 = 1400 psia. Unfortunately, this peak value is still much too low, below 0.003. As expected, case B shows a marked improvement over case A, but nevertheless η_c still remains below 0.01. Even the extremely optimistic case C gives a peak cycle efficiency of less than 0.04.

The efficiency curve for case C has an interesting bimodal form with the solution above p_1 = 1000 psia quite different from that below this limit. The analysis shows that the ejector cannot function for case C for values of p_1 above about 1000 psia, so the solution over this region pertains to a simple EHD conversion in a single stream; the ejector principle cannot be utilized in this region. It is ironic that the highest efficiency shown, nearly 0.04, occurs at about p_1 = 1400 psia where the fluid flywheel concept does not even apply! A second maximum cycle efficiency of about 0.026 occurs at p_1 = 270 psia. This point represents normal operation which utilizes the fluid flywheel principle to good advantage.

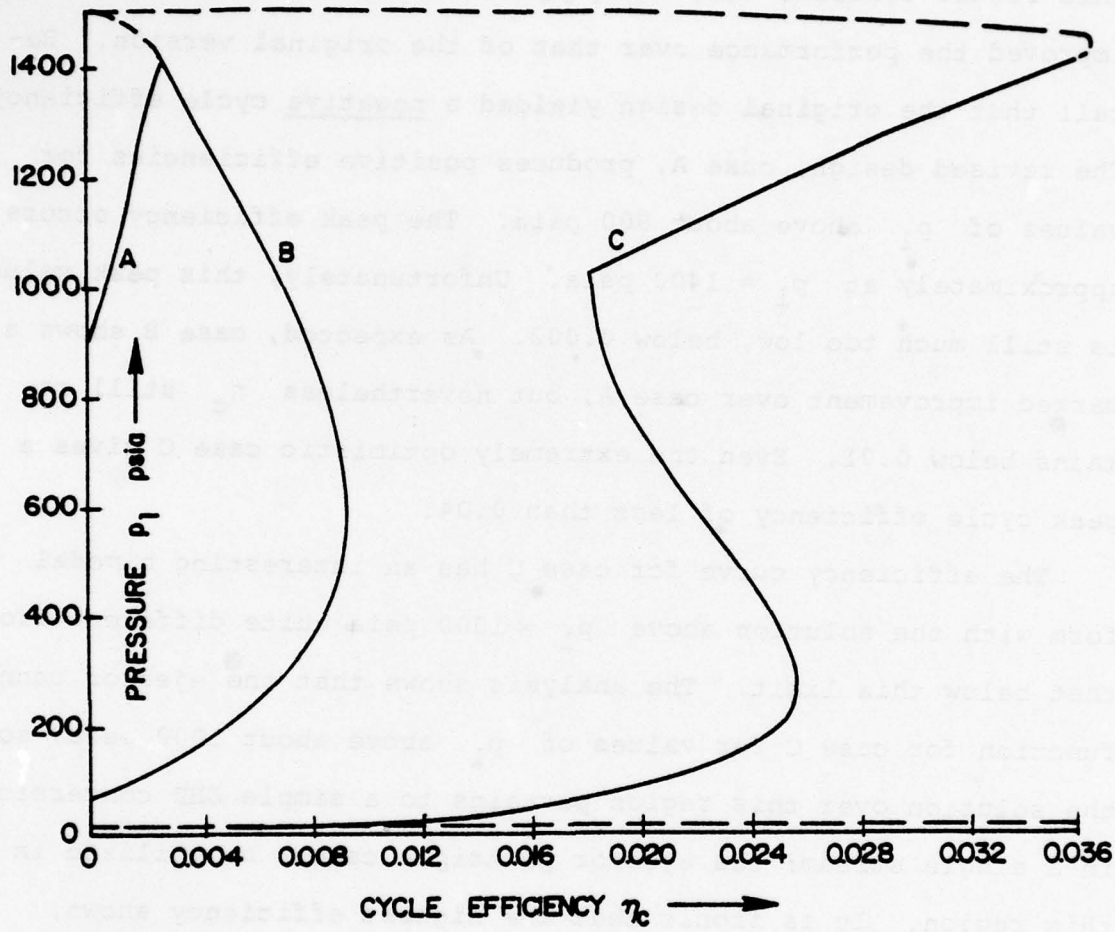

FIG 1A EFFICIENCY VERSUS PRESSURE AT STATION 1.

The results show that the final cycle efficiency that can be acheived, and the optimum back pressure p_1 and ejector area ratio (A_3/A_1) that will produce this optimum depend critically upon the three key parameters η_E, c_f and C_B. If these parameters can be estimated accurately then design optimization and resulting performance can be accurately predicted and controlled, otherwise not.

The results also show, however, that even under the most optimistic assumptions regarding η_E, c_f and C_B, the cycle efficiency is disappointingly low - less than 0.04! It is therefore clear that, viewed as a single stage device, the proposed EHD generator, even with the noted design improvements, has performance limitations which are just too severe to permit it to compete successfully with alternative power systems.

On the other hand, the possibility still remains that a multi-stage version of this generator might show a further order of magnitude improvement in performance. It is not clear at this time whether the ejector and fluid flywheel concepts can be incorporated to advantage in such a multi-stage design.

The remainder of this Appendix summarizes the analysis of the revised scheme. The notation and approach is generally similar to the main text. The derivations, formulas, tabulations and diagrams are complete but no attempt has been made to integrate them into a smooth flowing text.

ELECTRIC POWER COEFFICIENTS

$$\frac{P_e}{P_{K3}} = c_e = \nu y^2 \quad \text{where} \quad y = \left(\frac{V_1}{V_3}\right)$$

$$\frac{P_e}{P_{K1}} = K_e = \frac{\nu}{x} \quad \text{where} \quad x = \left(\frac{\dot{m}_1}{\dot{m}_3}\right)$$

$$\nu = 0.5837 \frac{\rho_1}{(h_o - h_i)} \quad \text{(CASES A \& B)}$$

ρ_1 = density, lbm/ft^3

$(h_o - h_1)$ = enthalpy drop, Btu/lbm

Note: Above constant 0.5837 is based on a value of the breakdown constant of:

$$C_B = 9.49 \times 10^3 \quad m^2 {}^\circ K/\text{coulomb}$$

An assumed increase in C_B by a factor $\sqrt{10}$ would increase ν by a factor of 10. This would give:

$$\nu = 5.837 \frac{\rho_1}{(h_o - h_1)} \quad \text{(CASE C)}$$

ENERGY BALANCE

OPERATING LIMIT

The fluid flywheel can function only if parameters η_E, c_f and ν satisfy the inequality

$$c_f\left(\frac{1}{\eta_E} - 1\right) + \nu\left(\frac{1}{\eta_E} + 1 + c_f\right) < 1 \tag{1}$$

OPERATING RANGE

Let

$$C_2 = \left(\frac{1}{\eta_E} - 1 + \nu\right) \tag{2}$$

$$C_1 = \frac{2}{\eta_E} \tag{3}$$

$$C_o = \left(\frac{1}{\eta_E} + 1 + c_f\right) \tag{4}$$

$$R^2 = C_1^2 - 4C_2C_o \tag{5}$$

A solution exists for any valve of y between the limits -

$$y_{min} = \left(\frac{C_1 - R}{2C_2}\right) \tag{6}$$

$$y_{max} = \left(\frac{C_1 + R}{2C_2}\right) \tag{7}$$

MASS RATIO x

The solution for mass ratio x is found by the following sequence of calculations.

$$A_1 = \frac{2(y - 1)^2}{\eta_E} \tag{8}$$

$$A_2 = \left(\frac{1}{\eta_E} - 1\right)y^2 \tag{9}$$

$$A_3 = \left(-\frac{1}{\eta_E} + 1 + c_f + \nu y^2\right) \tag{10}$$

$$B_2 = A_1 + (3 - 2y)A_2 + A_3 \tag{11}$$

$$B_1 = yA_1 - (y^2 - 3)A_2 + 2yA_3 \tag{12}$$

$$B_o = A_2 + y^2 A_3 \tag{13}$$

$$S^2 = B_1^2 - 4B_2B_o \tag{14}$$

$$x = \left(\frac{B_1 - S}{2B_2}\right) \tag{15}$$

Best performance corresponds to the minimum possible value of x. This is best found by numerical trial and error.

THERMODYNAMIC PARAMETERS

Let p = power, watts

p_{K1} = kinetic power at station 1, watts

Then $K = \frac{p}{p_{K2}}$ = power coefficient

$$K_e^* = \{1 + \frac{(T_4 - T_A)(s_o - s_4)}{(h_o - h_1)}\}$$ Reversible Electric Power

$$K_p^* = \frac{(p_o - p_4)v_4}{(h_o - h_1)}$$ Reversible Pump Power

$$K_Q = \{\frac{(h_o - h_4)}{(h_o - h_1)} - \frac{K_p^*}{\eta_p}\}$$ Heat Input

---

$$\frac{P''_e}{\dot{m}_1} = \{\frac{\eta_x{}^\nu}{x} - \frac{K_p^*}{\eta_p}\}(h_o - h_1)$$ Specific Output Watt Sec/Kg

$$\eta_c = \{\frac{\eta_x{}^\nu}{x} - \frac{K_p^*}{\eta_p}\}\frac{1}{K_Q}$$ Cycle Efficiency

---

PRINCIPAL PERFORMANCE PARAMETERS

Values used in calculations-

Excitation Factor $\frac{\eta_x{}^\nu}{x} = 1.00$

Pump Efficiency $\eta_p = 0.90$

THERMODYNAMIC PROPERTIES

$p_1 = p_4$ psia	t_o °F	$t_1 = t_4$ °F	v_1 ft^3/lbm	v_4 ft^3/lbm	h_o Btu/lbm	h_1 Btu/lbm	h_4 Btu/lbm	$s_o = s_1$ Btu/lbm °R	s_4 Btu/lbm °R
1400	596.23	587.10	0.2873	0.0231	1149.7	1144.7	598.7	1.3179	0.7963
1300	596.23	577.46	0.3140	0.0227	1159.7	1148.9	585.4	1.3273	0.7840
1200	597.28	567.22	0.3449	0.0223	1169.7	1152.8	571.7	1.3369	0.7711
1100	603.94	556.31	0.3812	0.0220	1180.7	1156.3	557.4	1.3470	0.7575
1000	611.16	544.61	0.4244	0.0216	1191.7	1159.3	542.4	1.3574	0.7430
900	619.6	531.98	0.4766	0.0212	1203.4	1162.0	526.6	1.3683	0.7275
800	629.66	518.23	0.5413	0.0209	1216.2	1164.2	509.7	1.3801	0.7108
700	641.50	503.10	0.6237	0.0205	1230.0	1165.7	491.5	1.3927	0.6925
600	655.9	486.21	0.7323	0.0201	1245.5	1166.6	471.6	1.4067	0.6720
500	673.79	467.01	0.8824	0.0197	1263.3	1166.6	449.4	1.4227	0.6487
400	697.24	444.59	1.1042	0.0193	1284.8	1165.5	424.0	1.4413	0.6214
300	729.7	417.33	1.4671	0.01890	1311.8	1162.4	393.84	1.4643	0.5879
200	779.33	381.79	2.1745	0.01839	1349.2	1156.2	355.36	1.4952	0.5435
100	877.29	327.81	4.2113	0.01774	1415.0	1142.8	298.40	1.5462	0.4740
14.696	1228.7	212.00	25.461	0.01672	1623.3	1101.9	180.07	1.6844	0.3120

p_o = 1500 psia

Steam quality at state 1 = 0.950

THERMODYNAMIC COEFFICIENTS

p_1 psia	ν	K_e^*	K_Q	K_p^*	$(\frac{\Delta h}{\Delta H})$
1400	0.4063	54.94	110.1	0.0855	0.009590
1300	0.1721	26.53	53.09	0.0778	0.2071
1200	0.1001	17.65	35.30	0.0732	0.03241
1100	0.06274	12.75	25.47	0.0667	0.04680
1000	0.04244	10.04	19.97	0.0617	0.06214
900	0.02958	8.151	16.28	0.0568	0.07940
800	0.02073	6.769	13.53	0.0521	0.09973
700	0.01455	5.716	11.43	0.0472	0.1233
600	0.01010	4.876	9.762	0.0424	0.1513
500	0.006839	4.178	8.375	0.0377	0.1855
400	0.004430	3.574	7.179	0.0329	0.2288
300	0.002663	3.037	6.113	0.0281	0.2871
200	0.001391	2.537	5.124	0.0229	0.3702
100	0.0005091	2.016	4.083	0.0169	0.5211
14.696	0.00004396	1.374	2.726	0.0088	1.0000

Notes:

$$\Delta h = (h_o - h_1)$$

$$\Delta H = (h_o - h_1)_{p_1 = 14.676}$$

Since system is closed, atmospheric pressure $p_1 = 14.696$ psia has no particular significance but serves as a convenient, if arbitrary lower pressure limit for the cycle calculations.

RESULTS OF EJECTOR OPTIMIZATION

	CASE A			CASE B			CASE C		
pi	Y_{OPT}	X_{MIN}	$(X/Y_{OPT}) = (A_1/A_3)_{OPT}$	Y_{OPT}	X_{MIN}	$(x/y)_{OPT} = (A_1/A_3)_{OPT}$	Y_{OPT}	X_{MIN}	$(X/Y)_{OPT} = (A_1/A_3)_{OPT}$
1400	1.0000	1.0000	1.0000	2.07	0.9564	0.4620	1.0000	1.0000	1.0000
1300	2.755	0.8588	0.3117	2.555	0.5691	0.2227	1.0000	1.0000	1.0000
1200	3.115	0.6970	0.2238	2.81	0.3835	0.1365	1.0000	1.0000	1.0000
1100	3.40	0.5848	0.1720	3.025	0.2688	0.0888	1.0000	1.0000	1.0000
1000	3.675	0.5106	0.1390	3.2025	0.1996	0.0623	2.045	Q9764	0.4775
900	3.875	0.4565	0.1178	3.425	0.1524	0.0445	2.29	0.8070	0.3254
800	4.075	0.4146	0.1017	3.65	0.1179	0.0323	2.48	0.6459	0.2625
700				3.95	0.0924	0.0234	2.65	0.5053	0.1907
600				4.25	0.0728	0.0171	2.81	0.3861	0.1374
500				4.65	0.0574	0.0123	2.98	0.2871	0.0963
400				5.20	0.0450	0.0087	3.19	0.2061	0.0646
300				5.70	0.0349	0.0061	3.45	0.1412	0.0409
200				6.70	0.0265	0.0040	3.95	0.0896	0.0227
100				8.00	0.0194	0.0024	5.00	0.0485	0.0097
14.696				9.65	0.0144	0.0015	8.15	0.0187	0.0023

PRINCIPAL RESULTS

p_i psia	CASE A		CASE B		CASE C	
	η_c	$P''_e/\dot{m}_1$ KW SEC / Kg	η_c	$P''_e/\dot{m}_1$ KW SEC / Kg	η_c	$P''_e/\dot{m}_1$
1400	0.0028	3.61	0.0030	3.83	0.0360	46.14
1300	0.0022	2.86	0.0041	5.42	0.0308	41.05
1200	0.0018	2.45	0.0051	7.06	0.0260	36.14
1100	0.0013	1.88	0.0062	9.05	0.0217	31.40
1000	0.0007	1.09	0.0072	10.85	0.0183	27.59
900	0.0001	0.15	0.0080	12.61	0.0186	29.21
800	-0.0006	-0.96	0.0087	14.26	0.0194	31.82
700			0.0092	15.70	0.0206	35.22
600			0.0094	16.81	0.0220	39.35
500			0.0093	17.60	0.0234	44.17
400			0.0086	17.17	0.0248	49.50
300			0.0074	15.69	0.0257	54.79
200			0.0053	12.14	0.0253	58.27
100			0.0018	4.73	0.0211	54.57
14.696			-0.0067	-8.15	0.0050	16.65

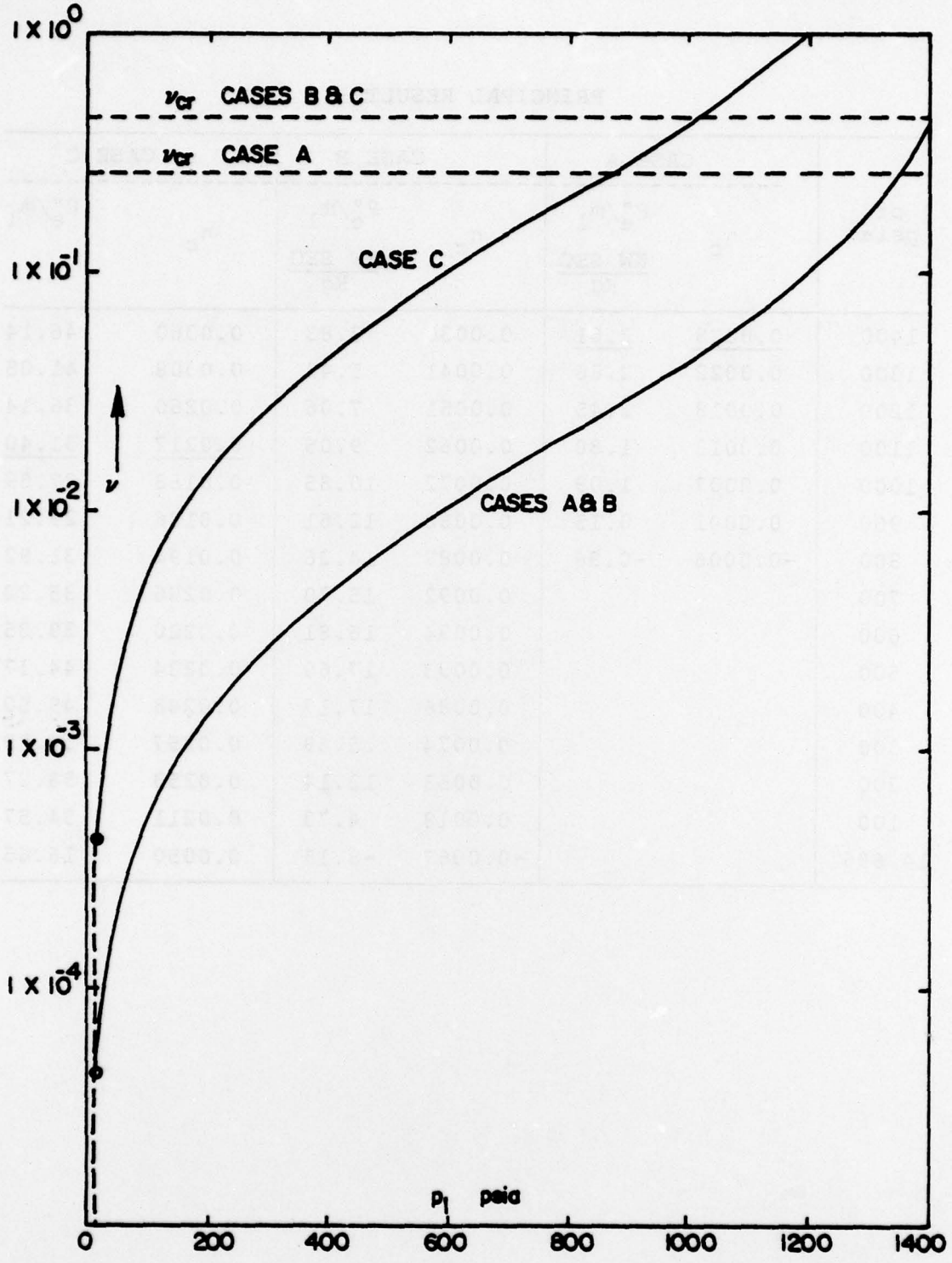

Fig. 2A ν versus pressure at station 1

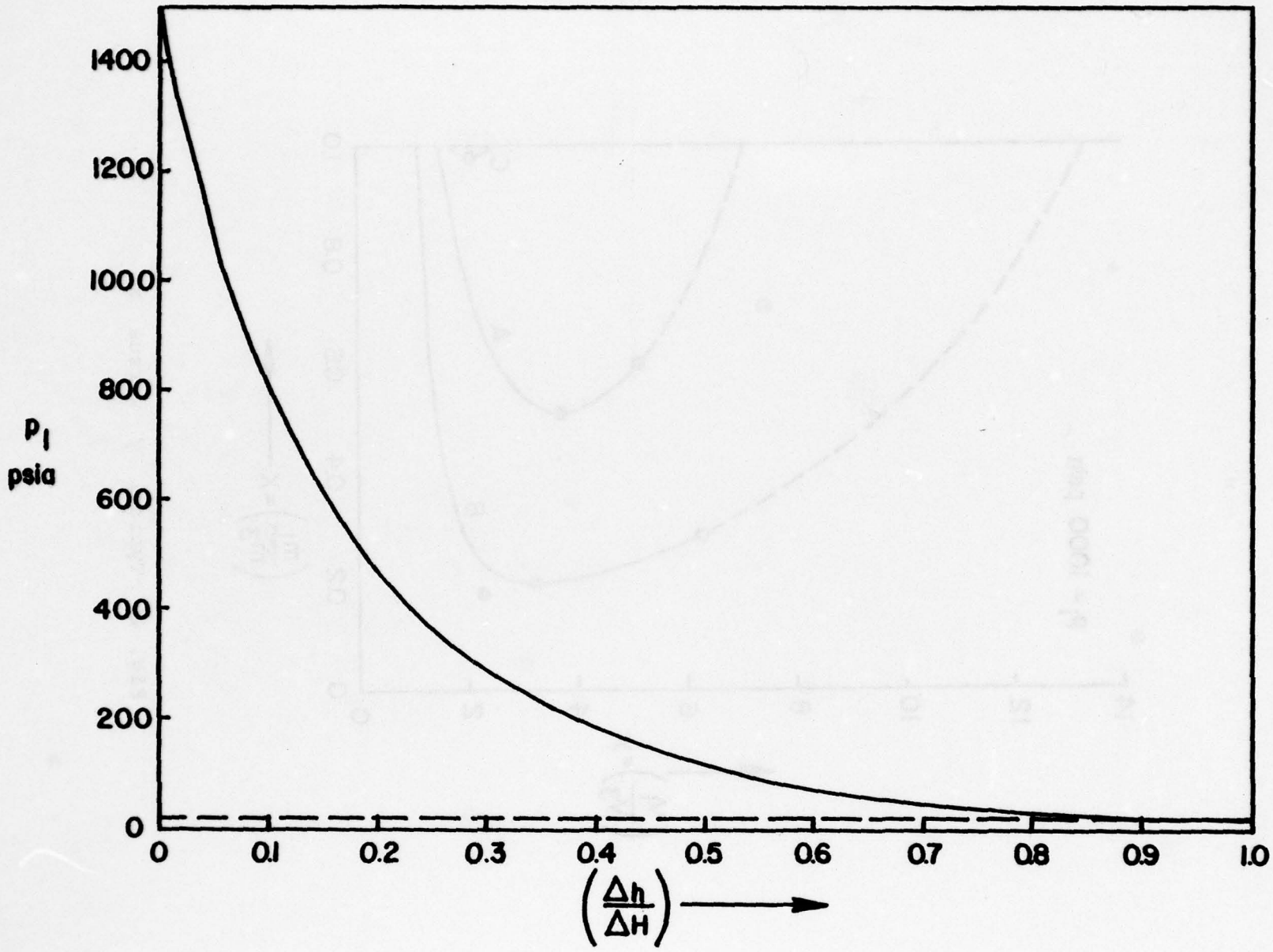

Fig. 3A Enthalpy Drop Relative to that at $p_1 = 14.696$

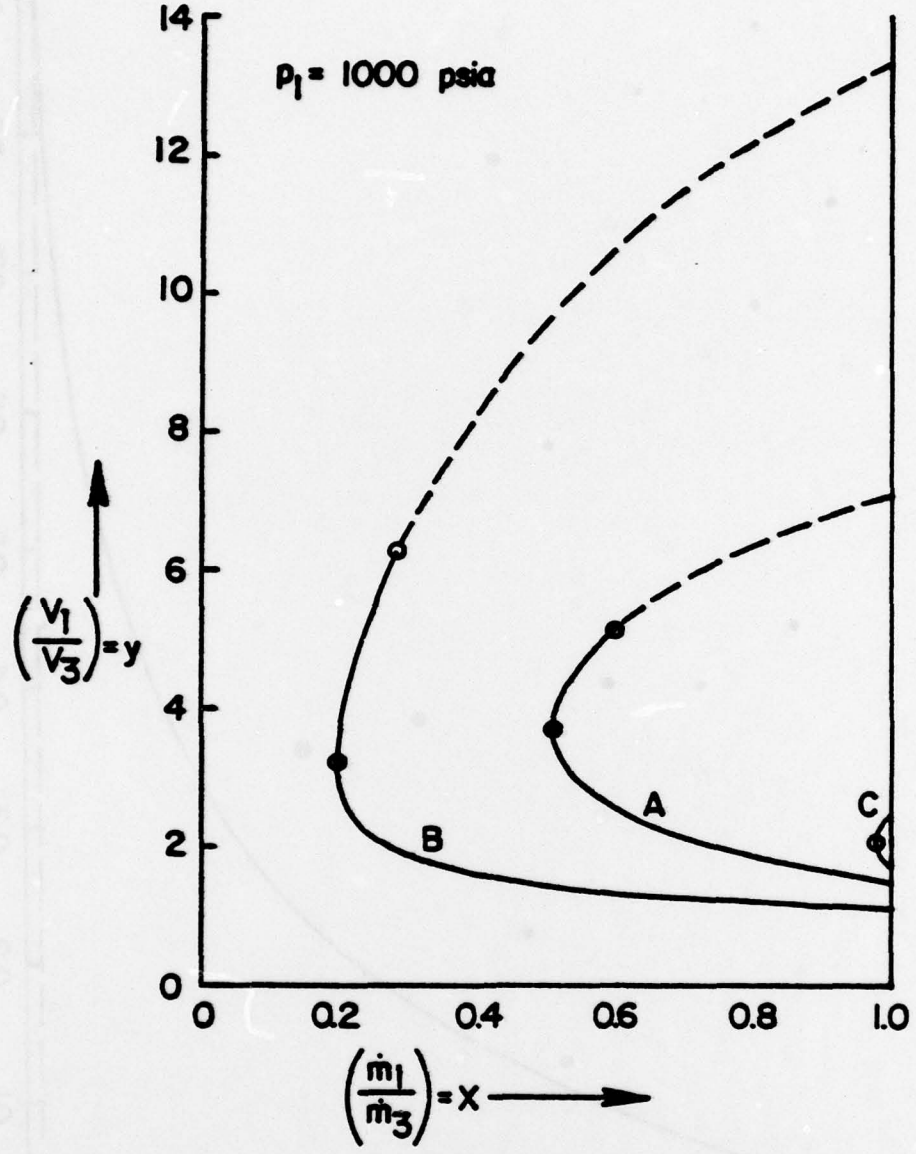

Fig. 4A Typical y versus x

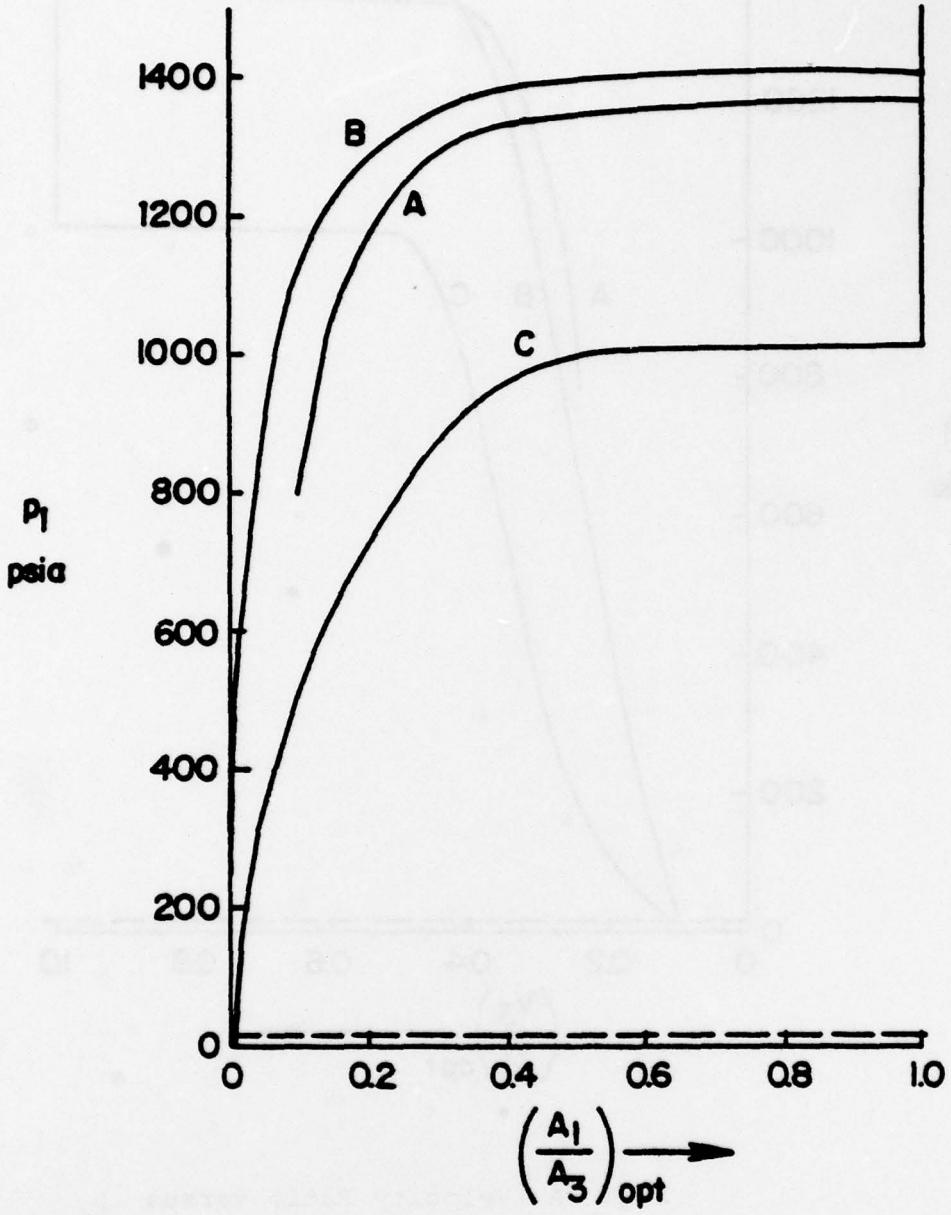

Fig. 5A Area Ratio versus p_1

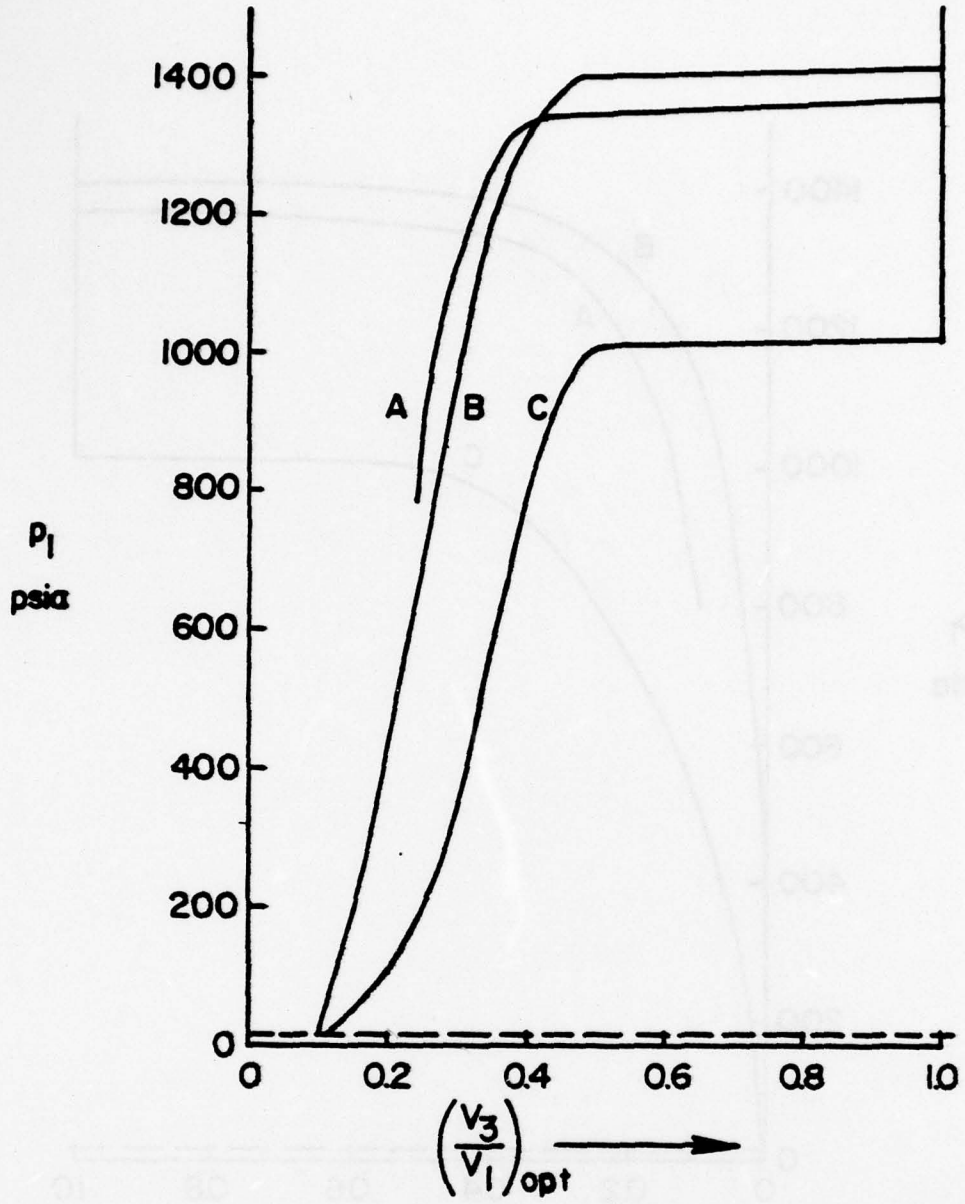

Fig. 6A Velocity Ratio versus p_1

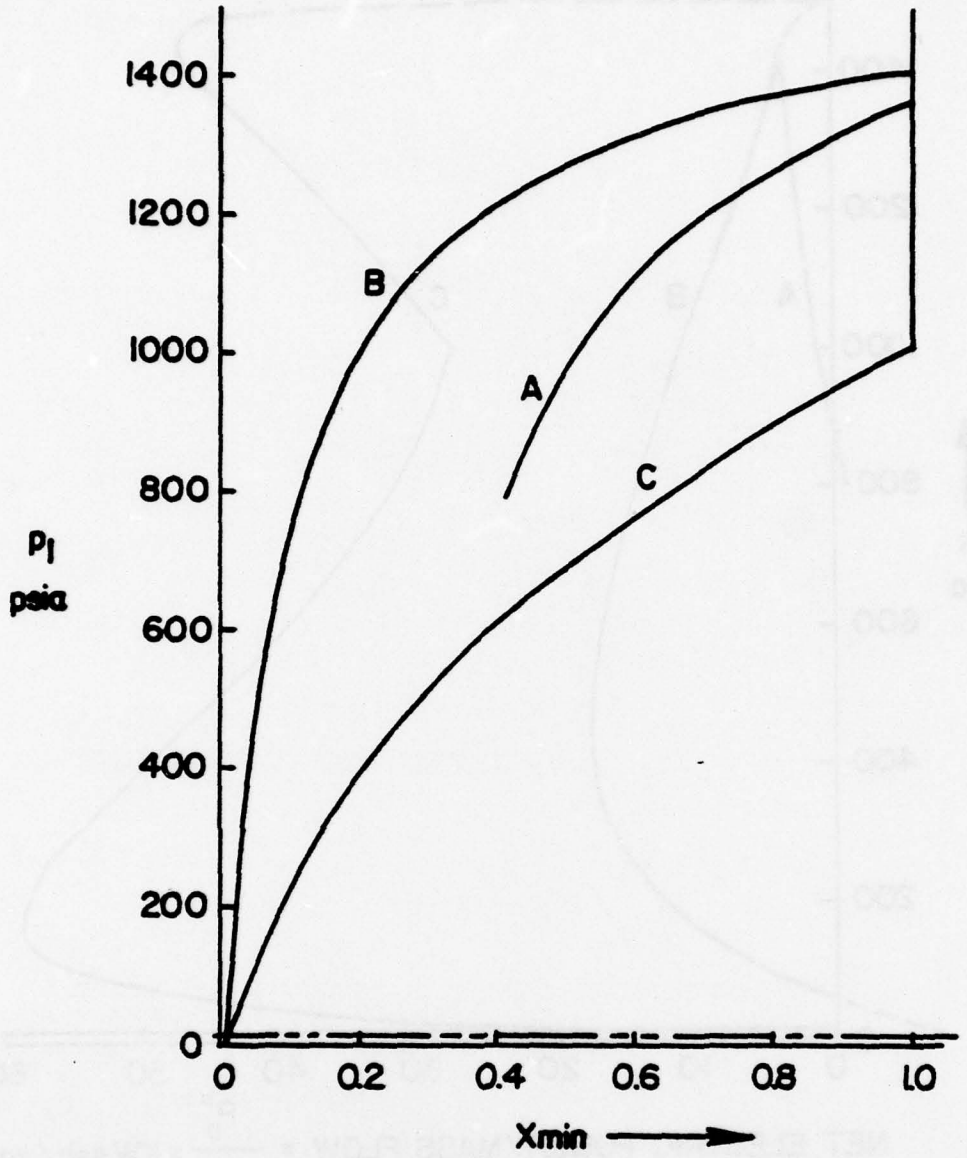

Fig. 7A Minimum Mass Ratio versus p_1

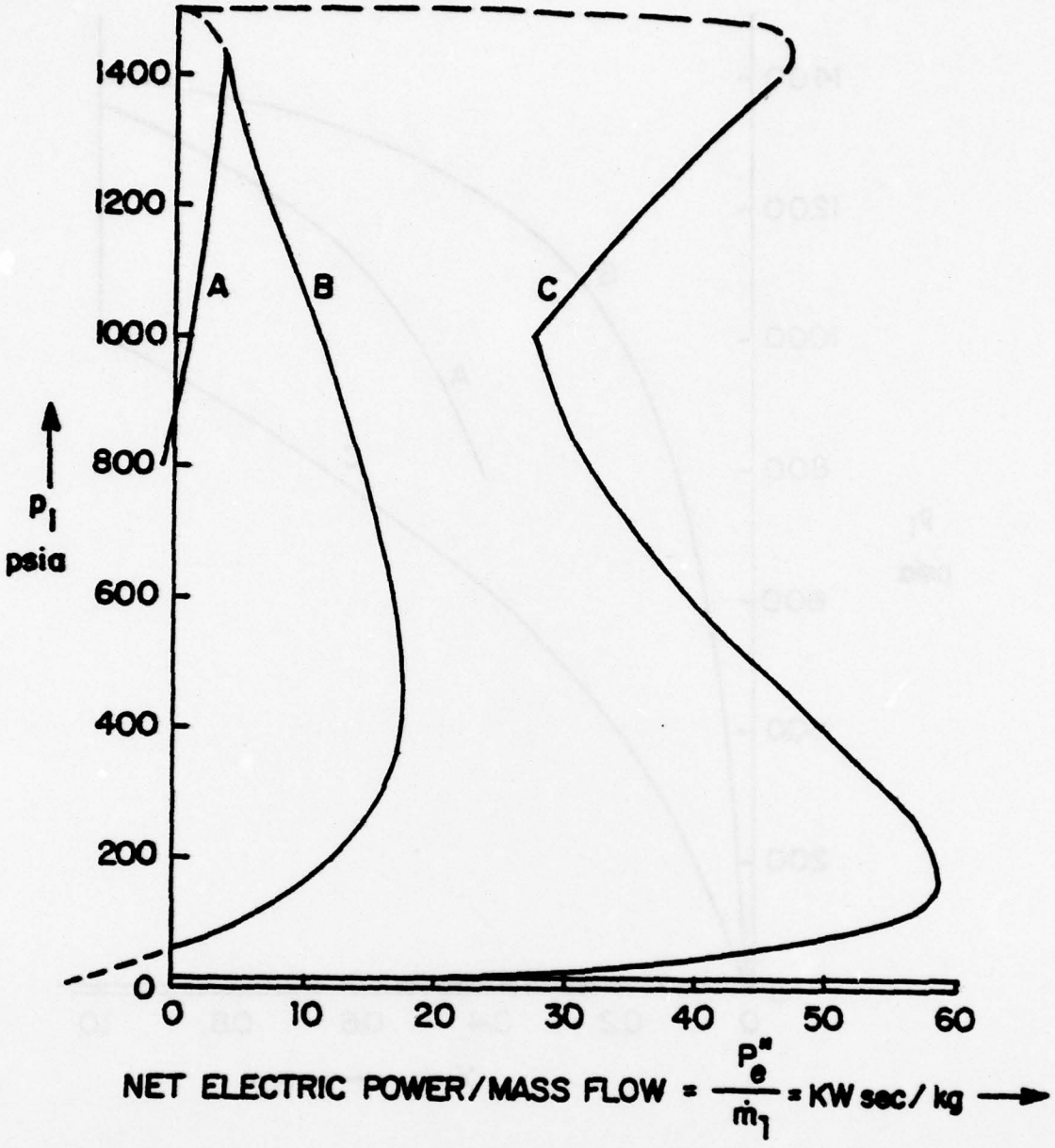

Fig. 8A Net Electric Power versus p_1

ELECTRIC POWER

$$\frac{P_e}{P_{K3}} = c_e = \frac{\frac{1}{2}\varepsilon C_B{}^2 R^2 \rho_3{}^2 A_3 V_3}{\frac{1}{2}\rho_3 V_3{}^3 A_3} = \frac{\varepsilon C_B{}^2 R^2 \rho_3}{V_3{}^2}$$

Also $\rho_3 = \rho_1$ and $V_3 = \frac{V_1}{y}$

$$\therefore c_e = \nu y^2 \text{ where } \nu = \frac{\varepsilon C_B{}^2 R^2 \rho_1}{V_1{}^2} = \frac{\varepsilon C_B{}^2 R^2 \rho_1}{2(h_o - h_1)}$$

Regrouping factors -

$$\nu = \left(\frac{\varepsilon C_B{}^2 R^2}{2}\right) \frac{\rho_1}{(h_o\ h_1)} \quad \text{(dimensionless)}$$

In metric units -

$$\left(\frac{\varepsilon C_B{}^2 R^2}{2}\right) = \frac{1}{2}\left[8.854 \times 10^{-12} \frac{\text{cmb}}{\text{vm}}\right]\left[9.49 \times 10^3 \frac{\text{m}^2\ ^\circ\text{K}}{\text{cmb}} \times 461 \frac{\text{J}}{\text{kg}\ ^\circ\text{K}}\right]^2$$

$$= 84.73\left(\frac{\text{Jm}^3}{\text{k}_g{}^2}\right)$$

In English units -

$$\left(\frac{\varepsilon C_B{}^2 R^2}{2}\right) = \left[84.73 \frac{\text{J}_m{}^3}{\text{k}_g{}^2}\right]\left[9.480 \times 10^{-4} \frac{\text{Btu}}{\text{J}}\right]$$

$$\times \left[3.281 \frac{\text{ft}}{\text{m}}\right]^3 \left[0.4536 \frac{\text{k}_g}{\text{lbm}}\right]^2$$

$$= 0.5837 \frac{\text{Btu ft}^3}{\text{lbm}}$$

Hence

$$\nu = 0.5837 \frac{\rho_1}{(h_o - h_1)} \quad \text{(dimensionless)}$$

where ρ_1 = density, lbm/ft^3

$(h_o - h_1)$ = enthalpy drop, Btu/lbm

also

$$\frac{P_e}{P_{K1}} = K_e = \frac{c_e}{xy^2} = \frac{\nu}{x}$$

SUMMARY

$$\nu = 0.5837 \frac{\rho_1}{(h_o - h_1)} \left\{ \begin{matrix} \rho_1 \\ (h_o - h_1) \end{matrix} \begin{matrix} \text{lbm/ft}^3 \\ \text{Btu/lbm} \end{matrix} \right\}$$

$$\frac{P_e}{P_{K3}} = c_e = \nu y^2$$

$$\frac{P_e}{P_{K1}} = K_e = \frac{\nu}{y}$$

ENERGY BALANCE

By a simple revision of previous work we obtain the two key equations.

$$\left(\frac{A1}{A3}\right) = \left(\frac{x}{y}\right) \tag{1}$$

$$\{xy^2 + \frac{(1-x)^3 y^2}{(y-x)^2} - 1\} - \frac{1}{\eta_E}\{xy^2 + \frac{(1-x)^3 y^2}{(y-x)^2} - 1 - \frac{2x(y-1)^2}{(y-x)}\}$$

$$- \{c_f + \nu y^2\} = 0 \tag{2}$$

Eq (2) can be reduced to the form:

$$A_1\{\frac{x}{y-x}\} - A_2\{x + \frac{(1-x)^3}{(y-x)^2}\} - A_3 = 0 \tag{3}$$

where

$$A_1 = \frac{2(y-1)^2}{\eta_E} \tag{4}$$

$$A_2 = (\frac{1}{\eta_E} - 1)y^2 \tag{5}$$

$$A_3 = (-\frac{1}{\eta_E} + 1 + c_f + \nu y^2) \tag{6}$$

Eq (3) can be further reduced to the form:

$$B_2 x^2 - B_1 x + B_o = 0 \tag{7}$$

$$B_2 = A_1 + (3 - 2y)A_2 + A_3 \tag{8}$$

$$B_1 = yA_1 - (y^2 - 3)A_2 + 2yA_3 \tag{9}$$

$$B_0 = A_2 + y^2 A_3 \tag{10}$$

Eq (7) may be solved by the quadratic formula. The larger of the two roots is extraneous and may be dropped.

$$\text{Let} \quad S^2 = B_1^2 - 4B_2B_o \tag{11}$$

$$\text{Then} \quad X = \left(\frac{B_1 - S}{2B_2}\right) \tag{12}$$

For the limiting case x = 1, Eq (2) reduces to the form:

$$C_2 y^2 - C_1 y + C_o = 0 \tag{13}$$

where

$$C_2 = (\frac{1}{\eta_E} - 1 + \nu) \tag{14}$$

$$C_1 = \frac{2}{\eta_E} \tag{15}$$

$$C_o = (\frac{1}{\eta_E} + 1 + c_f) \tag{16}$$

Let $$R^2 = C_1^2 - 4C_2C_o \tag{17}$$

The corresponding roots are:

$$y_{min} = (\frac{C_1 - R}{2C_2}) \tag{18}$$

$$y_{max} = (\frac{C_1 + R}{2C_2}) \tag{19}$$

The above roots are real only if R^2 is not negative. This will be the case if and only if:

$$c_f(\frac{1}{\eta_E} - 1) + \nu(\frac{1}{\eta_E} + 1 + c_f) \leq 1 \tag{20}$$

DISTRIBUTION LIST

		No. of Copies
1.	Defense Documentation Center Cameron Station Alexandria, Virginia 22314	2
2.	Library Code 0212 Naval Postgraduate School Monterey, California 93940	2
3.	Office of Research Administration Code 012A Naval Postgraduate School Monterey, California 93940	1
4.	Chairman Department of Aeronautics Code 67 Naval Postgraduate School Monterey, California 93940	1
5.	Dr. H. R. Rosenwasser Naval Air Systems Command Code AIR 310C Washington, D. C. 20360	1
6.	Mr. S. A. Satkowski Office of Naval Research Power Program, Code 473 Washington, D. C. 20360	1
7.	Dr. S. Hasinger Thermomechanics Branch AFFDL Wright-Patterson AFB, Ohio 45433	1
8.	Dr. C. D. Hendricks Lawrence Livermore Laboratory L-482 P.O. Box 808 Livermore, California 94550	1
9.	Dr. H. Velkoff Department of Mechanical Engineering Ohio State University Columbus, Ohio 43210	1

10. Dr. Ryszard Gajewski — 2
Division of Advanced Energy Projects
Mail Stop J-309
Department of Energy
Washington, D. C. 20545

11. Mr. Alvin Marks — 3
Dr. E. Y. Tsiang
Marks Polorized Corporation
153-16 10th Avenue
Whitestone, N.Y. 11357

12. Mr. M. O. Lawson — 1
University of Dayton Research Insitute
Dayton, Ohio 45469

13. Prof. T. H. Gawain — 2
Department of Aeronautics
Code 67Gn
Naval Postgraduate School
Monterey, California 93940

14. Prof. O. Biblarz — 5
Department of Aeronautics
Code 67Bi
Naval Postgraduate School
Monterey, California 93940

15. Dr. Hans von Ohain — 1
c/o
University of Dayton Research Institute
Dayton, Ohio 45469

16. Dr. J. R. Melcher — 1
Department of Electrical Engineering
Room 36-319
Massachusetts Institute of Technology
Cambridge, Massachusetts 02139

17. Prof. P. F. Pucci — 1
Department of Mechanical Engineering
Code 69 Pc
Naval Postgraduate School
Monterey, California 93940

18. Dr. Ernesto Barreto — 1
Atmospheric Research Center
State University of New York
130 Saratoga Road
Scotia, New York 12302